

*PHOTOIONIZATION OF GASES AND VAPORS
BY VACUUM ULTRAVIOLET RADIATION*

F. I. VILESOV

Usp. Fiz. Nauk 81, 669-738 (December, 1963)

TABLE OF CONTENTS

1. Introduction	888
2. Initial experiments	889
3. Methods of quantitative study of photoionization	889
4. Variation of the photoionization efficiency near the appearance thresholds of ions.	891
5. The semi-empirical method of calculating the ionization potentials of organic compounds	893
6. Photoionization cross-sections of atoms and simple molecules	894
7. The relation of the first adiabatic ionization potentials to the structures of molecules	895
8. Ionization potentials and electronic absorption spectra of organic compounds.	907
9. Mass-spectrometric study of photoionization processes	909
10. Kinetic-energy distribution of electrons in photoionization of aromatic compounds	910
11. Sensitized photoionization	915
12. Summary of the first adiabatic ionization potentials of molecular gases and vapors.	925
Bibliography	925

1. INTRODUCTION

IN recent years, interest has grown considerably in the problems of the interaction of vacuum far-ultraviolet radiation with matter. Among other problems, much attention has been paid to studying processes of photoionization of isolated atoms and molecules, i.e., gases and vapors at low pressures, in order to get quantitative information, which is most necessary in solving a number of other problems. For example, such data are necessary in understanding the photochemical and photoelectric processes that occur in the upper layers of the atmosphere,^[1] the processes of formation and maintenance of the ionized layers in the stratosphere,^[2] gas-discharge phenomena,^[3] etc.

The study of photoionization permits us to obtain the most reliable and precise values for adiabatic ionization potentials. These potentials, being one of the fundamental energy characteristics of isolated molecules, are widely used to get a deeper understanding of the structures of the latter. Along with the other physical and chemical constants characterizing the electronic structures of molecules as a whole, as well as the individual functional groups and chemical bonds, the ionization potentials undergo regular changes in chromatological series of compounds, and can be used to estimate electron affinities, electron-charge distributions, and the mutual influences of various functional groups in molecules.

Among the practical applications, I must point out that one can use photoionization to prepare sensitive stable detectors for vacuum ultraviolet radiation,^[4] to identify different isomers,^[5,8] and to generate ions

in ion sources in mass spectrometers designed for isotopic and chemical analyses in complex organic mixtures.^[6-8]

While the photoionization of monatomic gases (mainly the vapors of the alkali metals, which have low ionization potentials) had advanced to the stage of quantitative study as early as the thirties, studies on the photoionization of complex organic compounds and the simple gases have arrived at the stage of quantitative measurements only in recent years. The main reason why studies on photoionization of molecules have lagged lies in difficulties of the experimental type. The ionization potentials of most molecules have values of 8-12 eV or greater. This corresponds to the region of far vacuum ultraviolet radiation from $\lambda = 1400-1000 \text{ \AA}$ and shorter. Here even thin layers of air are completely opaque. We should bear in mind the fact that the best types of fluorite are transparent to 1250 \AA , and lithium fluoride to 1050 \AA . Thus, in the region of shorter wavelengths we must give up having vacuum windows between the light source, the spectroscopic apparatus, and the ionization cuvette. This creates difficulties in applying differential evacuation to the apparatus.

More than thirty years have elapsed since the publication of the only Russian-language review on photoionization of gases and vapors, by A. N. Terenin.^[9] During this time, and especially in the last five to seven years, much research has been conducted on the determination of precise values of ionization potentials, effective photoionization cross-sections, and the study of various processes connected with photoionization. Several review articles on photoionization^[10-13] and

on spectroscopy in the vacuum ultraviolet region of the spectrum^[14-18] have appeared in recent years in foreign literature.

In this review I shall try to discuss the studies on photoionization of complex organic compounds, to present briefly some data on the photoionization of atoms and simple molecules, since the latter have been the object of detailed discussion by Weissler,^[12] and to give as complete as possible a table of the first adiabatic ionization potentials of molecules, as obtained by various methods.

2. INITIAL EXPERIMENTS

The initial attempts to detect the photoionization of inorganic gases began with the studies of Lenard^[19] published in 1900-1902. In these studies he tried to show the existence of photoionization in air, oxygen, hydrogen, and carbon dioxide upon illuminating them with ultraviolet light that had been transmitted by a layer of air and the quartz windows of the apparatus. However, the results of these experiments aroused a series of well-grounded objections, and later Bloch^[20] showed in 1908 that the conductivity in these gases is due to a photoeffect on the tiny dust particles suspended in the irradiated volume, rather than to ejection of electrons from molecules.

The photoionization of air by the far-ultraviolet radiation of a hydrogen lamp, transmitted through a calcium fluoride window, was first observed by Hughes^[21] in 1910. He also established that if one replaces the fluorite window with a plate of crystalline quartz of thickness 0.3 mm, the ionization completely vanishes. Hence, the long-wavelength limit for photoionization of air lies within the region 1250-1450 Å. A number of other authors confirmed this result somewhat later, e.g.^[22-24]

Now, the first ionization potentials of oxygen, nitrogen, and carbon dioxide occur in a wavelength region considerably shorter than 1250 Å^[12] (O₂ — 990 Å, N₂ — 790 Å, CO₂ — 860 Å). Hence, in order to explain the observed phenomenon, Hughes^[25] suggested that the ionization is a cumulative process. Here the light absorption first brings a molecule into an excited metastable state. The ejection of an electron occurs when an already-excited molecule absorbs a new light quantum, or two excited molecules collide. This suggestion is not without some basis. Thus, for example, two metastable levels are known for molecular nitrogen: A³Σ_u⁺ having an energy of 6.2 eV, and a'(¹Σ_u⁻) having an energy of about 8.0-8.1 eV. If we ascribe the photoionization to the first triplet level A³Σ_u⁺, as is most probable, and take into account the exact value of the first ionization potential of molecular nitrogen, 15.576 eV,^[26] then to eject an electron from a molecule excited to this level will require an energy quantum of 9.3 eV. This corresponds to a wavelength of 1330 Å, in agreement with the early experiments. In

the case of oxygen, there are also two metastable levels, ¹Δ_g and ¹Σ_g⁺,^[27] having energies of about 1.0 and 1.7 eV. However, in this case the existence of these levels cannot explain the stepwise ionization as it does for nitrogen or mercury,^[28] since the ionization potential of molecular oxygen according to the most recent data is 12.15 eV.^[12] Consequently, to eject an electron from an excited molecule will require an energy quantum greater than 10 eV, corresponding to radiation of wavelength less than 1200 Å. Such radiation cannot be transmitted by fluorite, and hence the photoionization in dry air observed in the cited experiments can be explained only by the stepwise photoionization of molecular nitrogen or by the ionization of some products of photochemical reactions that might be formed upon irradiation of air by the far-ultraviolet radiation.

The study of the photoionization of organic vapors began with the researches of Stark^[29] and Serkov.^[30] Both authors observed an increase in the conductivity of the vapors of certain aromatic amines and other cyclic compounds upon irradiation with the ultraviolet radiation of a quartz mercury lamp that had been transmitted by a layer of air. When the pressure of the vapor being studied was increased, the conductivity rose to a maximum and then dropped. On the basis of his experimental results, Stark advanced the hypothesis that photoionization was taking place, and its observed yield declines at high pressures owing to an increase in the probability of electron-ion recombination.

While later studies have not confirmed the results of these experiments and their interpretation,^[31,32] they were the first attempt to detect directly the ionization of rather complex organic molecules by large light quanta using a method that has been widely developed in recent years on the basis of a new experimental technique.

3. METHODS OF QUANTITATIVE STUDY OF PHOTOIONIZATION

The quantitative studies of photoionization of gases and vapors include the determination of the values of the effective photoionization cross-sections of atoms or molecules, and of the adiabatic and vertical ionization potentials. The first adiabatic ionization potential is taken to mean the minimum energy necessary to ionize a molecule occurring in the ground state with the zero-level vibrational energy to form a positive ion in the ground state on the zeroth vibrational level. The higher adiabatic ionization potentials correspond to transitions to one of the excited electronic states of the ion having the zero-level vibrational energy. Here one assumes that the ejected electron has zero kinetic energy.

The fundamental experimental data for obtaining these values are the curves of the relation of the pho-

toionization yield to the energy of the acting photons. The photoionization yield is taken to mean the ratio of the ion current i to the amount of absorbed radiation $I_0 - I$, where I_0 and I are, respectively, the light fluxes of the incident and transmitted radiation in the ionization cuvette. If the ion current is measured in units of electrons/sec, and the absorbed radiation in quanta/sec, this ratio represents the absolute photoionization quantum yield (A). In practice, one also often uses a quantity 100 times as great, which is the number of ions formed per hundred absorbed photons.

The product of the absolute photoionization quantum yield A and the total effective absorption cross-section σ is the effective photoionization cross-section σ_i . The total absorption cross-section can be found from the well-known Lambert-Beer law

$$I = I_0 e^{-\sigma n_0 l \frac{p}{760} \frac{273}{T}},$$

where $n_0 = 2.687 \times 10^{19}$ molecules/cm³ (Loschmidt's number), l is the length of the absorption chamber in cm, p is the pressure in mm Hg, and T is the temperature in degrees Kelvin. When the pressure of the gas being studied is low (10^{-3} – 10^{-5} mm Hg) and the ionization cuvette is short, the photoionization cross-sections, which we shall simply call the photoionization efficiency below for the sake of brevity, are expressed by the ratio of the ion current to the acting light flux in photons/sec. In fact,

$$\sigma_i(\lambda) = A\sigma(\lambda) = \frac{i\sigma(\lambda)}{I_0(1 - e^{-\sigma n_0 l \frac{p}{760} \frac{273}{T}})}$$

and when $p \ll 1$,

$$e^{-\sigma(\lambda) n_0 l \frac{p}{760} \frac{273}{T}} = 1 - \sigma(\lambda) p l \frac{273}{760 T}$$

and

$$\sigma_i(\lambda) = \frac{i\sigma(\lambda)}{I_0\sigma(\lambda)l \frac{p}{760} \frac{273}{T}} = C \frac{i}{I_0},$$

where C is a constant coefficient depending on the instrumental parameters and the conditions of experiment.

At present, three methods are in use to measure the ionization potentials of atoms and molecules: the electron-impact method, using mass-spectrometric technique, the method of electronic absorption spectra in the far vacuum ultraviolet, and the photoionization method.

The determination of the ionization potentials corresponding to a process of elementary ionization according to the equation $AB + E \rightarrow AB^+ + e$ by the electron-impact method consists in determining the curve for the efficiency of ionization by electrons, with subsequent extrapolation to the intersection with the axis representing the energy of the ionizing electrons. The problem of extrapolating the ionization-efficiency curve for molecular gases to the value corresponding to the

first adiabatic ionization potential has a long history. Several methods^[33,34] have been proposed at various times, but none of them can be considered perfect or completely well-grounded. In most cases the stated extrapolations give higher values for the ionization potential than the first adiabatic ionization potentials determined by the spectroscopic or photoionization methods. While granting that the electron-impact method has such undoubted merits as its relative simplicity and universality, I must point out a number of technical and theoretical difficulties which reduce the accuracy and reliability of the results obtained. These include instrumental errors due to contact potential differences between the electrodes accelerating the electrons, and the lack of equipotentiality of the field in the ionization chamber, as well as the thermal velocity distribution of the electrons emitted by the hot cathode, which obeys a Maxwell-Boltzmann distribution, but is considerably distorted as the electrons pass through the entrance slit of the ionization chamber.^[35] These defects not only introduce a constant error in the measurement of the energy of the ionizing electrons, but also lead to a large dispersion in the energies of the electrons, which is difficult to measure. Even when one uses a comparative method (choosing as standard a gas whose ionization potential is known with high accuracy), the defects cannot be completely eliminated. The small ionization yield near the appearance threshold of the ions and the highly differing nature of the ionization-efficiency curves for different substances keep us from establishing a strict physically-grounded criterion for picking out the point on the ionization curve corresponding to the first adiabatic ionization potential.

Price and his associates^[36-39,41,45] have determined the first adiabatic ionization potentials of many compounds from an analysis of electronic-vibrational absorption spectra in the far ultraviolet. This method of determining the ionization potentials consists in finding the limits of convergence of Rydberg's series of bands, which are described by the formula

$$\nu_n = a - \frac{R}{(n+b)^2},$$

where $n = 1, 2, 3, \dots, \infty$. This method permits one to obtain values of adiabatic ionization potentials with an accuracy of the order of 0.01–0.001 eV. However, it is far from universally applicable, since the great complexity and diffuseness of the spectra of most complex organic molecules make it impossible to identify unambiguously the positions of the Rydberg bands.

The photoionization method, which has been recently developed, amounts in practice to determining the curve for the photoionization yield or efficiency and finding the point on it corresponding to the first adiabatic ionization potential. Just like the electron-impact method, it can be applied to measure the ionization potentials of any compounds whatever, regardless of the

nature of the absorption spectra, and at the same time, it furnishes data of a high accuracy (0.01–0.03 eV) comparable with that of the spectroscopic determination of the ionization potentials.

Compared with the electron-impact method, the photoionization method has two essential advantages:

1) It is much easier to get a monochromatic beam of photons with a strictly controlled energy than of electrons. Thus, for example, with ordinary vacuum monochromators one can easily obtain a resolution of the order of 1 Å, which corresponds in the photoionization region to a scatter of photon energies of the order of 0.01 eV.

2) In photoionization, the ion current near the appearance threshold of the ions rises very sharply, in distinction from ionization by electron impact. This difference is explained by the fact that the ionizing electrons, having spent their energy in ionization and in imparting a certain excitation to the ions, remain in their vicinity and can neutralize them.^[16] The ionization yield increases only when the excess kinetic energy becomes large enough that the electron and the ion swiftly separate.

In recent years, the photoionization technique has taken a new advance in development, namely, the study of the products of photoionization using mass-spectrometric technique,^[42,44,46,6,7] and the study of the energy spectra of the electrons ejected in photoionization.^[47,48] These make it possible to study in greater detail processes of dissociative photoionization and processes of distribution of the photon energy in excess of the adiabatic ionization potential between the positive ion formed and the ejected electron.

4. VARIATION OF THE PHOTOIONIZATION EFFICIENCY NEAR THE APPEARANCE THRESHOLD OF THE IONS

Theoretical treatment of variation in the efficiency of photoionization^[49,50] and ionization by electron impact^[49,51] in the region where the energy of the ionizing photons or electrons exceeds the ionization potential by several eV has shown that the ionization-efficiency as a function of the excess energy is an order of magnitude smaller for photoionization than for ionization by electrons. When photoionization proceeds only from a single level of the molecule to a single level of the ion, the threshold law for the ionization efficiency is expressed by a step function (a Heaviside function). The photoionization efficiency is zero when $E - I_p < 0$; here E is the energy of the photon and I_p is the ionization potential of the atom or molecule. A jump occurs when $E = I_p$, and it remains constant for $E - I_p > 0$. Under analogous conditions in electron-impact ionization, the ionization-efficiency function $f_e(E - I_p)$ is a linear function of the excess energy of the electrons beginning at the value $E = I_p$,

i.e.,

$$f_e(E - I_p) = K_e(E - I_p).$$

A number of experimental investigations of the photoionization cross-sections of simple molecules and atoms have been made,^[52-57] and they agree satisfactorily with these ideas. For illustration, Fig. 1 gives the curves for the variation of the effective photoionization cross-section σ_i and the total absorption cross-section σ of nitric oxide.^[52] The curve of the photoionization cross-section as a function of the wavelength of the ionizing radiations shows several well-marked steps corresponding to the positions of the vibrational levels of the ion. The portion of the curve within the limits of one vibrational level is well defined by a step function. The jump in σ_i at longest wavelength corresponds to the transition from the zero vibrational level of the ground state of the molecule to the zero vibrational level of the ground state of the molecular ion. Hence it is the adiabatic ionization potential of nitric oxide. The other steps on the σ_i curve correspond to transitions to the higher vibrational levels of the ion. While the absorption spectrum σ consists of a greater number of bands that are very hard to identify, we can easily find from an analysis of the σ_i curve the positions of the vibrational levels of the positive ion (the spacings between the steps on the wavelength axis) and the probabilities of the transitions of the molecule from the ground state to the corresponding vibrational level of the ion (the height of the steps).

In the ionization of more complex molecules, the curves for the efficiency and yield of ionization become considerably more complex, since at temperatures considerably above 0°K (room temperature) the molecules always have a supply of vibrational energy. Here the occupancy of the vibrational levels approximately obeys the Boltzmann law. That is, it is proportional

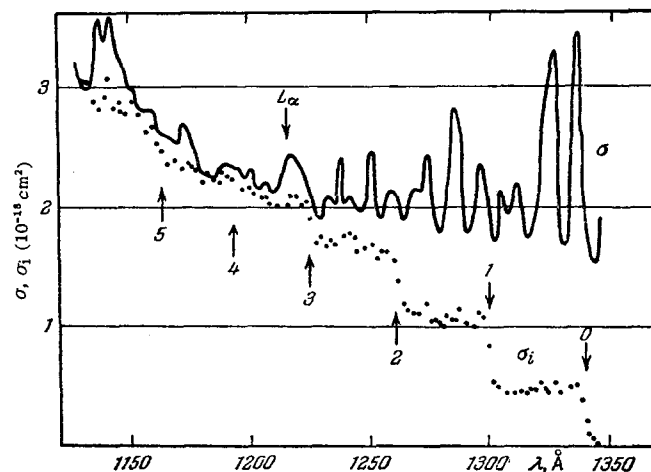


FIG. 1. Total absorption cross-sections σ and photoionization cross-sections σ_i of nitric oxide.^[52]

to $\exp(-\Delta E/kT)$. Ionization from these vibrational levels gives rise to an ion current at photon energies lower than the first adiabatic ionization potential, which corresponds to the 0-0 transition. Here, if the probabilities of ionization from all vibrational levels are equal, the increase in the photoionization efficiency must follow an exponential law. As a rule, these levels are not resolved, and hence, the ionization originating from them results in a smearing-out of the abrupt jumps in the ion current, both in the region of the adiabatic ionization potential and in the region of the transitions to the various excited levels of the ion.

Watanabe^[52] has discussed in detail the ionization-yield curves near the appearance threshold of the ion current, and has formulated a physically-grounded criterion for finding the adiabatic ionization potentials from them. He was the first to show that the low-energy tails of the photoionization-yield curves of molecules are exponential in nature. Figure 2 shows the curves of the photoionization yields of CS_2 and CH_3I ^[52] drawn on a semilogarithmic scale. We see from Fig. 2 that the long-wavelength tails can be approximated by straight lines. The breaks in these curves correspond to the first adiabatic ionization potentials. Watanabe calculated the ionization yields from the vibrational levels of the ground state of the molecules under the assumption that the levels are occupied according to the Boltzmann law ($T = 300^\circ\text{K}$) and that the probabilities of ionization from all levels are the same. The points marked by crosses correspond to the calculated values; we see that they agree well with the experimental curves.

In the region of the ionization continuum, the ionization yield varies more smoothly, and the nature of the variation is determined by the structure of the energy levels and the probability of transitions to them. One can show that the degree of the ionization-efficiency function can be greater than unity in the photoionization case, and greater than two in photoionization

by electrons, if one takes into account the set of vibrational levels in the ion. We shall discuss the case in which all the molecules have zero-point vibrational energy, and transitions from the zero level of the molecule to all vibrational levels of the ground state of the ion are equally probable, the latter levels being separated by equal spacings. Then, if the threshold law for the probability of transition to a particular vibrational state of the ion is given by a Heaviside function, we will obtain a first-degree function in photoionization in the region of the ionization continuum. Actually, with a great number of vibrational levels in the ion, we obtain in the limit for photoionization

$$f_{\text{ph}}(E - I_p) |_{E - I_p > 0} = \int_0^{E - I_p} K_{\text{ph}} d(E - I_p) = K_{\text{ph}}(E - I_p).$$

An analogous treatment in ionization by electrons gives a second-degree function:

$$f_e(E - I_p) |_{E - I_p > 0} = \int_0^{E - I_p} K_e(E - I_p) d(E - I_p) = \frac{1}{2} K_e(E - I_p)^2.$$

When the probability of transition to the higher vibrational levels is smaller than to the lowest level, corresponding to the case in which the interatomic distances in the molecule and the ion differ little (Fig. 3a), the degree of the ionization-efficiency function will be a fraction between zero and unity for photoionization, and will be between unity and two for ionization by electrons. In the converse case, in which the probability of transition to the higher levels is greater, corresponding to the case of differing interatomic distances in the ion and the molecule (Fig. 3b), the degree of the function for photoionization will be greater than unity, and for ionization by electrons, greater than two. We should now take into account the fact that the total absorption cross-sections of complex molecules vary little in a region of the ionization continuum corresponding to transition to a single electronic state of the ion. Hence the relation $\sigma_1 = \sigma A$ implies that all that has been said above about the effective ionization cross-sections holds true also for the ionization yield.

The experimental results obtained by a number of authors^[44, 52, 58, 59] agree well with one another and with

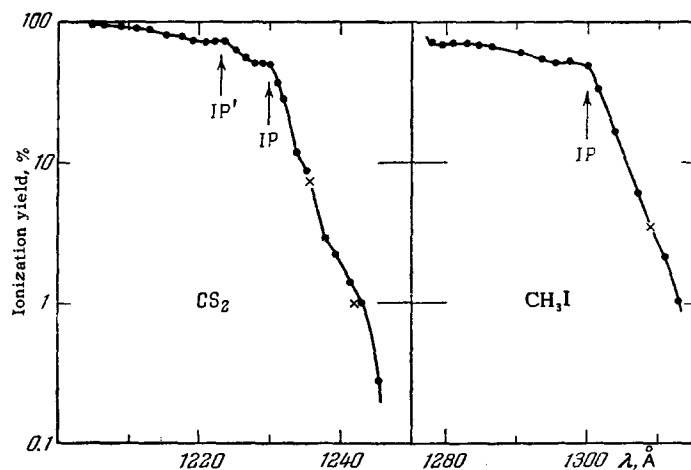


FIG. 2. Photoionization-yield curves of carbon disulfide and methyl iodide.^[52]

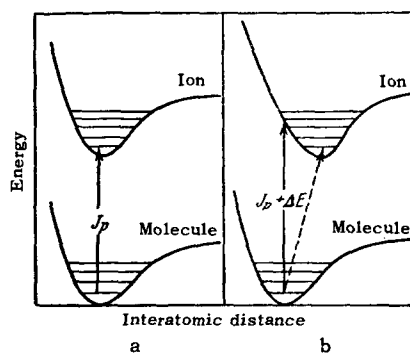
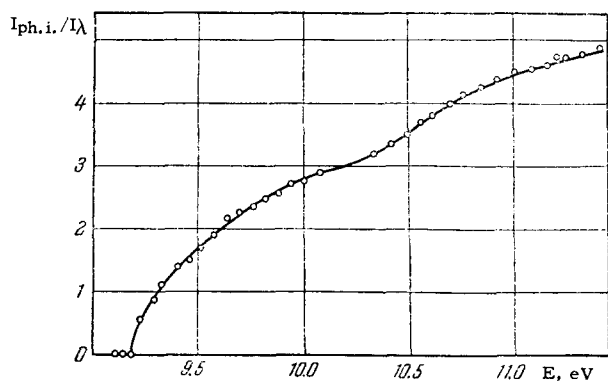


FIG. 3. Potential curves illustrating ionization transitions.


 FIG. 4. Photoionization-efficiency curve of benzene.^[59]

the ideas presented above on the increase in the ionization efficiency in the region of photon energies exceeding the adiabatic ionization potential of the molecule by several eV. Figures 4 and 5 give the photoionization-efficiency curves of benzene and aniline. For benzene, for which the interatomic distances do not vary or vary little upon ionization, the most probable transition is the one from the zero vibrational level of the molecule to the zero vibrational level of the ion, and the function for the efficiency of ionization by photons has an exponent of degree less than unity. That is, we observe an abrupt increase in the ion current at the ionization threshold, which tapers off as the photon energy is increased. In the photoionization of aniline, the interatomic distances differ appreciably, as we can see, and the degree of the function is higher. Figures 6 and 7 give the photoionization-yield curves for these same compounds on a semilogarithmic scale, as obtained with a higher energy resolution of the photons.

The ideas presented here and the experimental results show that the break in the curve, where the exponential section of the curve, arising from the ionization of vibrationally-excited molecules, goes over into the smoother (approximately first-degree) section of the curve in the region of the ionization continuum, arising from transitions to the excited vibrational levels of the ion, marks the adiabatic ionization potential of the molecule.

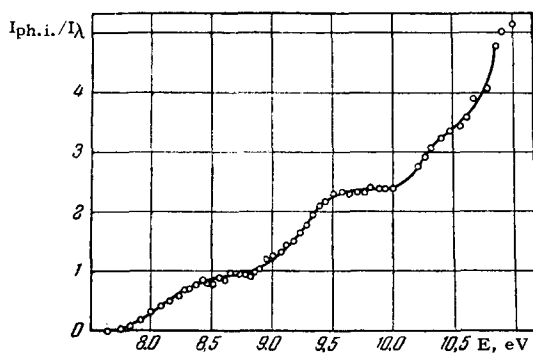
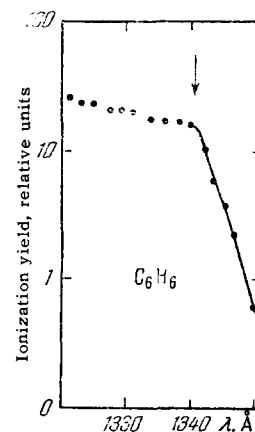

 FIG. 5. Photoionization curve of aniline.^[59]

 FIG. 6. Photoionization-yield curve of benzene.^[52]


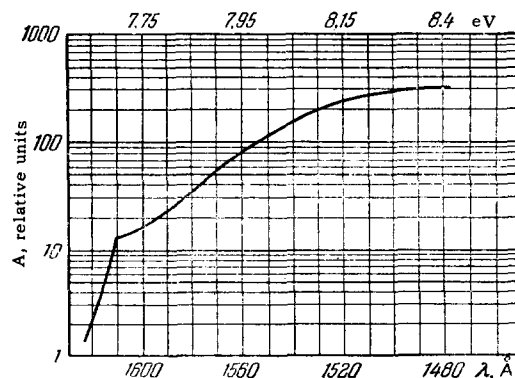
If transitions occur to several electronic states of the ion in the region of photon energies being studied, then, provided that the enumerated conditions are fulfilled, the photoionization-efficiency curve will be found, to a first approximation, to take the form of a sequence of linear segments with increasing slopes with respect to the energy axis. The breakpoints will correspond to the higher adiabatic ionization potentials.

5. THE SEMI-EMPIRICAL METHOD OF CALCULATING THE IONIZATION POTENTIALS OF ORGANIC COMPOUNDS

Exact theoretical calculations of ionization potentials are very complex, even for simple atoms. Semi-empirical calculations of ionization potentials of organic compounds were first carried out by Hall^[60] and by Lennard-Jones and Hall^[61] using the method of equivalent orbitals. If the molecular orbitals do not overlap, this method leads to a solution of the secular determinant

$$|l_{m,n} - E\delta_{m,n}| = 0,$$

where m and n refer to electrons in different bonds of the molecule. The roots of this determinant are the ionization potentials of the molecule; the smallest root corresponds to the first ionization potential, which is usually determined from experiment.


 FIG. 7. Photoionization-yield curve of aniline.^[110]

ejecting electrons. The curves of the photoionization cross-sections as a function of the energy of the ionizing photons near the appearance threshold of the ions can be satisfactorily represented as step functions.

In the cases of argon,^[72] neon,^[73] thallium,^[74] indium,^[75] etc., diffuse lines appear in the region of the ionization continuum. These lines can be unequivocally interpreted as being preionization lines from higher-energy transitions. For example, in argon the two systems of transitions $3p \rightarrow ms$ and $3p \rightarrow md$ ($m =$ quantum number) correspond to two states of the ion: $^2P_{3/2}^0$, having an ionization threshold at 786.72 \AA ; and $^2P_{1/2}^0$ at 777.96 \AA , respectively. The levels of the transitions occurring between these states of the ion are broadened, owing to the additional probability of transitions into the ionization continuum.

In the region of the ionization continuum, the values of the effective cross-sections obtained from direct experimental measurements do not remain constant as the wavelength of the acting radiation varies. Figure 8 gives some curves showing the relation of σ_i to the energy of the ionizing photons for certain monatomic gases and vapors according to Weissler.^[12] For argon, helium, and lithium, the photoionization cross-sections decrease monotonically with increasing energy quanta; the extent of decrease for a 1 eV change in the energy quantum is relatively small. In the photoionization of Na and Cs, σ_i first falls rapidly to a certain minimum, and then rises just as rapidly.

The theoretical calculations of the photoionization cross-sections of atoms give values agreeing satisfactorily with the experimental data. We can see this from Table I, which gives the experimental and calcu-

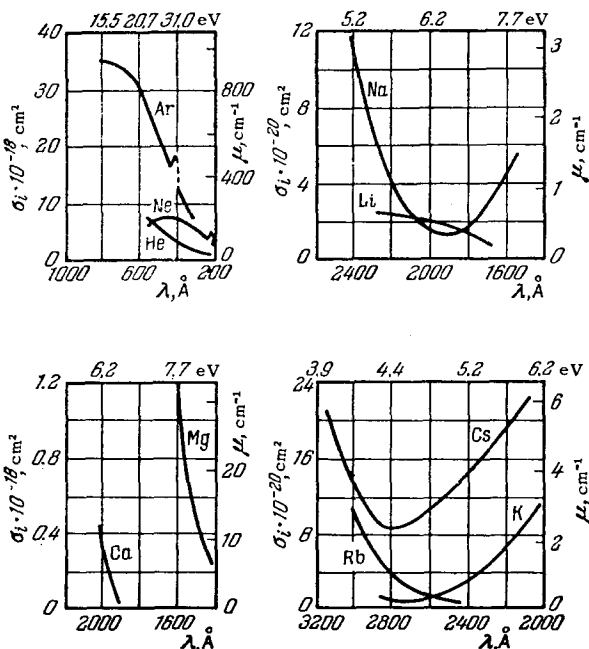


FIG. 8. Photoionization cross-sections of monatomic gases and vapors.^[12]

lated values of σ_i for certain wavelengths and indicates how they vary.

The curves of the effective photoionization cross-sections of diatomic and triatomic molecules are more complex in nature. They cannot be completely described on the basis of a threshold law in the form of a step function, even if we take into account the vibrational levels of the ions. Peaks are clearly shown at certain photon energies, with ionization cross-section values much greater than in the continuum. The most distinct peaks of this kind were recently found in a study by Weissler,^[46] who investigated the relative photoionization cross-sections of simple gases using a mass-spectrometric analysis of the ionization products (O_2 , N_2 , CO , CO_2 , NO , etc.) and in an analogous study^[57] on the photoionization of Br_2 , I_2 , HI , and CH_3I , and also on the curves of the first derivative of the efficiency of ionization by electrons.^[76] In these studies the intense peaks in the ionization-continuum region were ascribed to autoionization processes. As with certain monatomic vapors, the primary process here, which is dependent on the photon energy, is excitation. This is followed by the energy-independent process of ionization. It has been shown in^[57] that in the case of autoionization, the law of variation of the ionization efficiency as a function of the photon energy is described by a δ -function. The superposition of step and δ -functions satisfactorily explains the experimental data.

Absolute values have not yet been obtained for the photoionization cross-sections of more complex compounds in the range of photon energies considerably above the first ionization potentials. The data on the absolute values of the ionization yield^[16,52] near the ionization threshold show that the ion yield progressively diminishes with increasing molecular dimensions. Price^[16] suggests that this may involve dissociation processes or internal conversion of the energy of the absorbed photon. The probability of such processes is increased in complex molecules, owing to the capture of the ejected electron by the molecule itself. The relative photoionization cross-sections for a large number of compounds were obtained in^[59,64] using a mass-spectrometric technique in a range of photon energies up to 11.7 eV. The photoionization-efficiency curves were rather smooth in form, but a number of cases exhibited certain irregularities, which were explained by excited electronic levels of the ions or by processes of dissociative ionization.

7. THE RELATION OF THE FIRST ADIABATIC IONIZATION POTENTIALS TO THE STRUCTURES OF MOLECULES

A vast material has been accumulated in recent years on the precise values of ionization potentials, obtained by the spectroscopic^[15] and photoionization methods.^[11,16] This has made it possible to establish

Table I

Sub-stance	Method	Spectral Region, Å	$\sigma_i, 10^{-18} \text{cm}^2$		Course of variation	Refer-ences
			At ioni-zation thresh-old	At min-imum		
Ar	Absorption spectra	850—350	36		σ_i decreases with increasing photon energy.	77, 55
	Theoretical calculation		30			77
	Simultaneous measurement of photoionization and absorption spectra	900—500	35		σ_i decreases with increasing photon energy.	78
Ne	Absorption spectra	700—230	5.5		σ_i has a maximum at 400 Å.	56
	Theoretical calculation		5.8		σ_i has a maximum at 400 Å.	79
			4.4			
He	Absorption spectra	600—250	7.3		σ_i decreases.	55
	Theoretical calculation		7.4		σ_i decreases.	80
			7.5		σ_i decreases.	81
Li	Absorption spectra	2400—1700	2.5		σ_i decreases.	67
	Theoretical calculation		3.6		σ_i decreases.	82
			2.9		σ_i has a maximum at 1900 Å.	83
			1.16		σ_i smoothly increases.	84
Na	Absorption spectra	2500—1600	0.116	1900 Å	σ_i decreases to a minimum, then increases.	54
	Theor. calc.		0.10	0.013	Analogous course.	85
			0.07	10^{-5}		
K	Absorption spectra	3000—1600	0.12	2700 Å	σ_i increases beyond a minimum.	68
	Theor. calc.			0.008	Analogous course.	85
Rb	Photoionization	3000—2500	0.11	0.004	σ_i decreases to a minimum.	71
	Theor. calc.			0.004		85
	Photoionization	3200—2400	0.23	2800 Å	σ_i increases beyond a minimum.	71
Cs	Absorption spectra	3300—2000	0.22	0.043	Analogous course.	53
	Theor. calc.			0.078		85
				0.03		
Mg	Theor. calc.	1650—1450	8.2		σ_i decreases.	86
	Absorption spectra		1.2		σ_i decreases.	70
Ca	Absorption spectra	2100—1950	0.45		σ_i decreases.	69
	Theor. calc.		25		Analogous course.	87
In	Absorption spectra	2140—1758	0.3		Strong preionization.	68
Tl	Absorption spectra	2100—1450	4.5		Strong preionization.	74
N	Absorption spectra	800—400	10		σ_i almost constant, with maximum value = 12.5.	88
	Theoretical calculation		10		Analogous course, with maximum value = 10.08 at 650 Å.	89
			2.8		$\sigma_i = 13$ at 550 Å.	80
O ₂	Photoionization and absorption spectra	1050—500			σ_i has a maximum value = 16 at 600 Å.	78, 90
N ₂	Photoionization and absorption spectra	800—500			σ_i has a maximum value = 24 at $\lambda = 750$ Å.	78, 90
H ₂	Photoionization and absorption spectra	850—650			σ_i has a maximum value = 9 at $\lambda = 750$ Å.	78

Table I (cont'd)

Substance	Method	Spectral Region, Å	$\sigma_i, 10^{-18} \text{ cm}^2$		Course of variation	References
			At ionization threshold	At minimum		
CO	Photoionization and absorption spectra	900—470			σ_i has a maximum value = 32 at $\lambda = 650 \text{ Å}$.	78
NO	Photoionization and absorption spectra	1600—1050			σ_i increases.	52, 91
N ₂ O	Photoionization and absorption spectra	970—680			Maximum $\sigma_i = 27$ at $\lambda = 700 \text{ Å}$; strong preionization at $\lambda = 833 \text{ Å}$, with $\sigma_i = 60$.	91
NH ₃	Photoionization and absorption spectra	1240—680			σ_i has a maximum value = 31 at $\lambda = 700 \text{ Å}$.	92
CH ₄	Photoionization and absorption spectra	1000—470			Maximum value of $\sigma_i = 2.1$ at the ionization threshold.	78
	Theoretical calculation				σ_i at the ionization threshold = 94.	77
H ₂ O	Photoionization and absorption spectra	1000—470			σ_i has a maximum value = 18 at $\lambda = 600 \text{ Å}$.	78
C ₂ H ₂	Photoionization and absorption spectra	1100—680			σ_i has a maximum value = 57 at $\lambda = 800 \text{ Å}$.	93
C ₂ H ₄	Photoionization and absorption spectra	1190—680			σ_i has a maximum value = 50 at $\lambda = 700 \text{ Å}$.	93

a direct relationship between the structures of molecules and the values of their ionization potentials, even to the point of establishing simple quantitative relationships in some cases.

Aliphatic hydrocarbons. The ionization potentials of the paraffins, as obtained by the spectroscopic and photoionization methods by Price,^[95] Watanabe,^[11] and other authors^[96] are given in the summary Table XVIII. Certain values of ionization potentials obtained by the electron-impact method are also given here. As a rule, they are 0.02–0.2 eV greater than the ionization potentials obtained by the optical methods. An analysis of the table shows that the first substitution of a hydrogen atom by a methyl group diminishes the ionization potential considerably. However, as the hydrocarbon chain is lengthened, the decline becomes slower and approaches saturation.

At present, the ionization potentials of the first seven members of the unbranched paraffins have been measured with an accuracy of 0.02–0.03 eV. Figure 9 shows their relation (open circles) to the number of carbon atoms in the chain. The ionization potentials of the compounds of this series can be represented by the simple formula

$$I_{pn} = 9.06 + \frac{7.42}{n} - \frac{4.56}{n^2}, \quad n = 1, 2, 3, \dots, \infty,$$

where n is the number of carbon atoms in the chain. The solid circles in Fig. 9 correspond to the ionization

potentials calculated from this formula. The deviation from the experimental data does not exceed 1%, except for methane, for which the ionization potential is almost 1 eV greater than the calculated value. This should not surprise us, since for methane the first ionization potential is due to the ejection of a σ -electron from a C–H bond,^[11] while in all the other compounds the σ -electrons of C–C bonds are ejected.^[97] If the given formula is valid for the higher members of

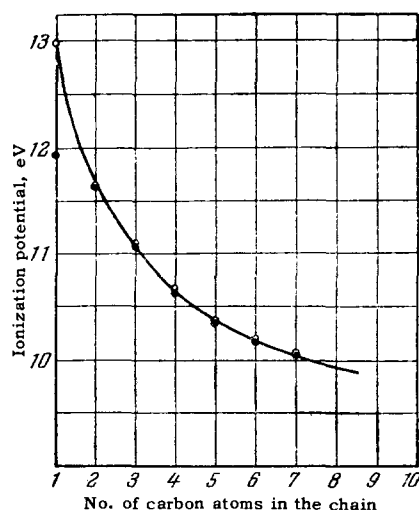


FIG. 9. Curve of the relation of the ionization potential to the number of carbon atoms in the linear hydrocarbons.

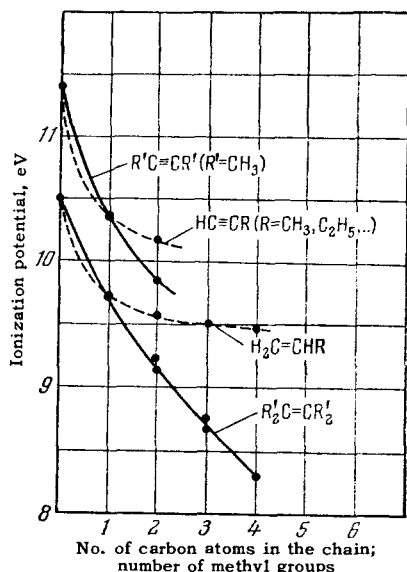


FIG. 10. Curves of the relation of the ionization potential to the structure of alkyl derivatives of ethylene and acetylene.

determined as follows. If we take the series of linear saturated hydrocarbons, the replacement of a hydrogen atom in a high enough member of the series by a methyl group should increase the heat of combustion by 157.4 kcal/mole, as has been shown in [98]. This value can be considered to be the contribution to the heat of combustion of the molecule upon replacement of a hydrogen atom by a methyl group under the condition that the interaction of the methyl group with the rest of the molecule is small. The difference between 157.4 kcal/mole and the experimentally observed heat of combustion is, to a first approximation, a measure of the interaction of the given methyl group with the rest of the molecule, and is called the stabilization energy S of the ground state of the molecule:

$$S = 157.4 - [C(\text{MX}) - C(\text{HX})] \text{ kcal/mole,}$$

where $C(\text{MX})$ is the heat of combustion of the methyl-substituted molecule, and $C(\text{HX})$ is the heat of combustion of the unsubstituted molecule. The stabilization energy thus calculated represents the energy shift of the ground state of the molecule upon replacement of one hydrogen atom by a methyl group in it. The stabilization energy S^* of the ion is defined as the sum of the stabilization energies of the molecule and the

change in the ionization potential upon substitution:

$$S^* = \Delta I_p + S.$$

Table IV gives the total stabilization energies of the unsaturated hydrocarbons with respect to ethylene and the stabilization energies of the corresponding ions. [16] The ionization-potential differences are also given here.

We see from Table IV that the ionization potentials vary considerably more than the stabilization energy of the ground state of the molecule. Here, as the ground state of the molecule is lowered, a decline in the ionization potential takes place, indicating a considerable drop in the ground state of the ion. The nature of such a considerable stabilization of the ion can be explained by the polarization of the alkyl groups by the positive hole in the double bond formed upon removal of one of the π -electrons. The size of this effect, as we see from Table IV, is a function of the "closeness of packing" of alkyl groups about the double bond. The quite considerable stabilization in the methyl derivatives of ethylene, of the order of several kcal/mole, can be explained by polarization effects between the electron-donor methyl groups and the π -electrons of the double bond.

For the saturated hydrocarbons, the stabilization energy of the ground state calculated in the same way is negligibly small. Hence, the interaction of the methyl groups with the rest of the molecule is insignificant here.

In the case of radicals, the stabilization energies of the ground and ionized states are close to the stabilization energies of the corresponding olefins. This indicates that the interaction of the unpaired electron with the methyl groups is of the same order of magnitude as in the olefin case.

The mutual influence of different functional groups in a molecule is commonly described qualitatively within the framework of the induction effect and the conjugation effect. [100] Within the framework of these effects, the decline in the ionization potentials of the alkyl derivatives of ethylene can be considered to be a positive induction effect of the alkyl groups on the ethylenic double bond. This effect is insignificant for molecules in the ground state, but increases with excitation, and attains a maximum with the positive ion. The action of these effects will be discussed in greater detail below, using the example of two classes of com-

Table IV. Stabilization energy of alkyl derivatives of ethylene (kcal/mole)

Compound	S	ΔI_p	S^*	Compound	S	ΔI_p	S^*
Propylene	2.67	18.0	20.6	Cis-2-butene	4.00	31.9	35.9
1-Butene	2.28	21.4	23.7	Trans-2-butene	5.1	31.9	37.0
1-Pentene	2.59	23.2	25.8	3-Methyl-2-butene	7.9	41.2	50.2
1-Hexene	2.60	24.2	26.8	2,3-Dimethyl-2-butene	8.7	51.0	59.8
Isobutylene	5.51	29.5	35.1				

Table V

Halogen atom \ R	H	CH ₃	C ₂ H ₅	<i>I</i> _p of the halogen atom [118]	Electronegativity of the halogen with respect to hydrogen [100]
Cl	12.85	11.28	10.97	12.96	0.8
Br	11.62	10.53	10.24	11.84	0.6
I	10.38	9.54	9.33	10.44	0.3

pounds for which there is a broader experimental material.

Halogen derivatives of the linear saturated hydrocarbons. The size of the induction effect for a particular electron-donor group increases proportionally upon introduction of substituents of greater electronegativity. In order to establish the linear relation between the induction effect and the changes in the ionization potentials, we shall discuss some data on halogen derivatives of the linear hydrocarbons. Their ionization potentials are given in Table V, from the data of [11].

In these compounds, the first ionization potential is due to the ejection of one of the *p*-electrons of the halogen atom. Just as for the alkyl derivatives of ethylene, there is an induction interaction here between the halogen atom and the alkyl group. Examination of the data of Table V and Fig. 11, which gives the curves of the variation of the ionization potentials for these compounds, shows that the ionization potential varies most for chlorine, which has the highest ionization potential and electron affinity; the variation is less for the bromine derivatives, and least for the iodine derivatives.

A more detailed examination shows that the ratio of the electronegativity differences between the alkyl group and the halogen atom is approximately equal to the ratio of ionization-potential differences. Thus, for methyl chloride and bromide, the ratio of the electronegativity differences between the methyl group and the corresponding halogen is 1.6, while the ratio of the ionization-potential differences ($I_p\text{-HCl} - I_p\text{-CH}_3\text{Cl}$) / ($I_p\text{-HBr} - I_p\text{-CH}_3\text{Br}$) is 1.5. If we bear in mind the fact that the electronegativities of atoms, and especially of atomic groups, are known at present to an accuracy of the order of 10–20%, such an agreement is quite satisfactory, and demonstrates the linear relation between the size of the induction effect and the change in the ionization potential of the molecule when one of its hydrogen atoms is replaced. This relation can be used to estimate the electronegativity of various functional groups in molecules.

Compounds containing the carbonyl group. Price and Walsh [38,97,101] have obtained the ionization potentials of certain simple aldehydes and ketones by the spectroscopic method, and have shown that in these compounds one of the *p*-electrons of the carbonyl oxygen

is ejected. Later, a great number of ketones, ethers, and certain of their halogen derivatives have been studied by the photoionization method, and their adiabatic ionization potentials were determined with high precision (0.01–0.03 eV). [11,58,102] These compounds are convenient objects for studying the law of variation of the mutual influences of functional groups in molecules as a function of the distance between them, since the electron to be ejected is localized in the vicinity of the carbonyl oxygen atom, and its ionization potential depends on the electron density in the vicinity of this atom.

Table VI gives the ionization potentials of a series of ketones arranged in an order such that each successive member of the series can be considered to be a methylated derivative of the preceding one. In this series of compounds, we observe a regular decline in the ionization potentials (Fig. 12), which can be explained by the positive induction effect (+I) of the alkyl groups on the carbonyl group. A more detailed examination shows that the ionization-potential differences between consecutive members of the series obey an inverse-square law with respect to the distance between the carbonyl group and the added methyl group, just as with the alkyl derivatives of ethylene. In fact, the replacement of a hydrogen atom in formaldehyde by a CH₃ group reduces the ionization potential by 0.7 eV. A second CH₃ group directly joined to the car-

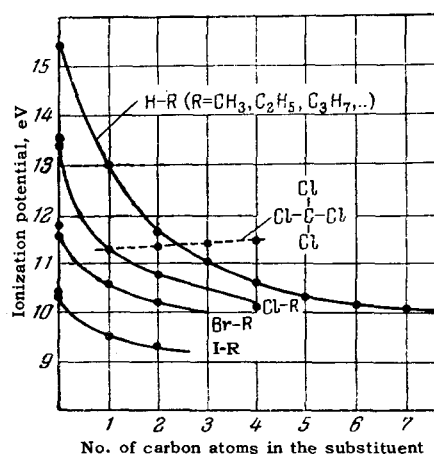


FIG. 11. Curves of the relation of the ionization potential to the structure of halogen derivatives of the linear saturated hydrocarbons.

Table VI. Ionization potentials of a series of ketones (eV)

Compound	Formula	Ionization potential	Ionization-potential difference
Formaldehyde	$H_2C=O$	10.90 ± 0.03	
Acetaldehyde	$\begin{array}{l} CH_3 \\ \diagdown \\ C=O \\ \diagup \\ H \end{array}$	10.20 ± 0.03	0.70
Acetone	$\begin{array}{l} CH_3 \\ \diagdown \\ C=O \\ \diagup \\ CH_3 \end{array}$	9.71 ± 0.03	0.51
Methyl ethyl ketone	$\begin{array}{l} CH_3 \\ \diagdown \\ C=O \\ \diagup \\ C_2H_5 \end{array}$	9.54 ± 0.03	0.17
Methyl propyl ketone	$\begin{array}{l} CH_3 \\ \diagdown \\ C=O \\ \diagup \\ C_3H_7 \end{array}$	9.47 ± 0.03	0.07
Methyl n-butyl ketone	$\begin{array}{l} CH_3 \\ \diagdown \\ C=O \\ \diagup \\ C_4H_9 \end{array}$	9.44 ± 0.03	—
Diethyl ketone	$(C_2H_5)_2C=O$	9.34 ± 0.02	0.16
Pinacolone	$\begin{array}{l} (CH_3)_3C \\ \diagdown \\ C=O \\ \diagup \\ CH_3 \end{array}$	9.18 ± 0.03	0.20
Ethyl tert-butyl ketone	$\begin{array}{l} (CH_3)_3C \\ \diagdown \\ C=O \\ \diagup \\ C_2H_5 \end{array}$	8.98 ± 0.02	0.16
Isopropyl tert-butyl ketone	$\begin{array}{l} (CH_3)_3C \\ \diagdown \\ C=O \\ \diagup \\ (CH_3)_2CH \end{array}$	8.82 ± 0.02	0.17
Pivalone	$\begin{array}{l} (CH_3)_3C \\ \diagdown \\ C=O \\ \diagup \\ (CH_3)_3C \end{array}$	8.65 ± 0.03	

bonyl carbon lowers the ionization potential further by 0.5 eV. If we replace one of the hydrogen atoms in dimethylketone by a CH_3 group, it will be twice as far away, and the decrease in the ionization potential should be one-fourth as great, as is observed experimentally. An analogous treatment can be extended to the higher members of the series. This makes it possible to write an approximate relation for the given series of ketones:

$$\Delta I_p \approx \frac{\text{const}}{l_{n+1}^2}$$

where ΔI_p is the difference in ionization potential between two consecutive members of the series; l_{n+1} is the relative distance between the carbonyl group and the hydrogen atom that is replaced by a methyl group to form the $(n+1)$ th member of the series.

If we assume that the ionization potentials in this series of ketones vary as a linear function of the induction effect, this implies that the induction interaction decreases in inverse proportion to the square of the distance between the methyl and carbonyl groups.

An examination of the ionization potentials of the more complex branched ketones given in the second half of the table shows that the inverse-square relation of the potential differences to the distance obeys an additivity rule quite accurately. In fact, pinacolone can be considered to be acetone in which three hydrogen atoms have been replaced by methyl groups. The re-

placement of a hydrogen atom by one methyl group in acetone decreases the ionization potential by 0.17 eV. This implies that the ionization potential of pinacolone should be 0.51 eV lower than that of acetone, i.e., 9.20

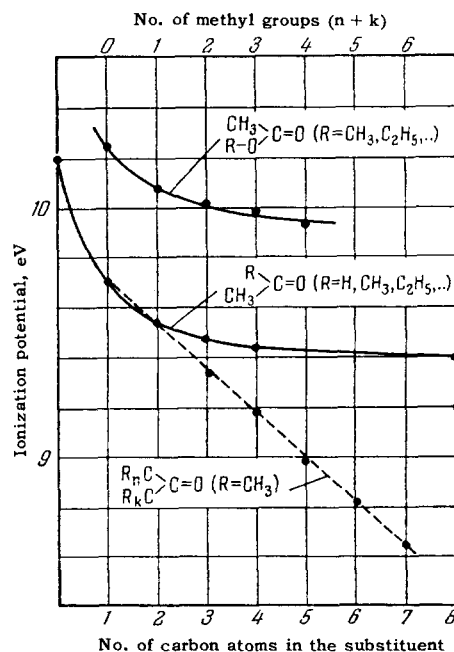


FIG. 12. Curves of the relation of the ionization potential to the structure of ketones and esters.

eV. From experiment we have 9.18 ± 0.03 eV. An analogous treatment for pivalone, which can be considered to be acetone in which all six hydrogen atoms have been replaced by methyl groups, gives an ionization potential of 8.69 eV; from experiment we have 8.65 ± 0.03 eV.

Certain deviations from these regularities occur in the ionization potentials for the first members of the series, in which the methyl groups are directly joined to the carbonyl carbon. They can be explained by a certain contribution from other types of interaction.

These regularities hold not only for the ketones, which show only the positive induction effect, but also for their halogen derivatives, which show a negative induction effect ($-I$) leading to an increase in the ionization potential of the p -electrons of the carbonyl oxygen. In fact, the ionization potential of chloroacetone is 9.91 ± 0.03 eV, and of dichloroacetone, 10.12 ± 0.03 eV, as measured in [102]. These values are respectively 0.20 and 0.41 eV higher than the ionization potential of acetone, which is 9.71 eV.

To illustrate the regularities under discussion, Fig. 12 shows some curves for the relation of the ionization potential to the number and position of the substituent CH_3 groups.

An examination of the first ionization potentials of esters, as obtained by the photoionization method, [103] shows that these compounds also obey well the regularities cited above. The ionization potentials of esters are higher than those of the corresponding ketones, indicating the lowering of the electron density in the vicinity of the carbonyl oxygen atom owing to the negative induction effect of the oxygen of the ester group. The ionization potentials of a series of esters having suc-

cessively longer alkyl chains in the ester group are compared with the corresponding ketones in Table VII. It shows that the ionization-potential difference is 0.55 eV, to an accuracy within the experimental limits of error of 0.02–0.03 eV. This clearly indicates the high additivity of the induction effects of opposite signs. When the alkyl group directly attached to the carbonyl carbon is lengthened, this difference becomes of the order of 0.45 eV. This non-equivalence of the different alkyl groups may be due to a weakening of the induction effect by the chain of conjugated bonds $-\text{O}-\text{C}=\text{O}$ or to a steric factor. Just as in the ketones, the additivity of the different induction effects is maintained also in the halogen derivatives of the esters. For illustration, Table VIII gives the ionization potentials of some chloro- and bromo-derivatives of esters.

The established regularities in the variation of the ionization potentials of ketones, esters, and their halogen derivatives can be successfully used to estimate first adiabatic ionization potentials with an accuracy no poorer than 0.05–0.1 eV.

Alkyl derivatives of benzene. Price and his associates [104–109] have measured the first ionization potentials of the monoalkyl and dialkyl derivatives of benzene with a precision as good as 0.01–0.005 eV, since these compounds exhibit sharp absorption bands arranged in Rydberg series. They showed that in these compounds the first ionization potentials arise from the ejection of one of the π -electrons of the benzene ring. Price explains the decrease in the ionization potential of benzene upon replacement of one or several of the hydrogen atoms by alkyl groups by the electron-donor character of the alkyl groups, which

Table VII. Ionization potentials of esters and ketones (eV)

Compound	Formula	I_p of the ester	I_p of the ketone	Difference (ΔI_p)
Ethyl acetate	$\begin{array}{c} \text{CH}_3 \\ \diagdown \\ \text{C}_2\text{H}_5-\text{O}-\text{C}=\text{O} \end{array}$	10.08 ± 0.02	9.54	0.54
n-Propyl acetate	$\begin{array}{c} \text{CH}_3 \\ \diagdown \\ \text{C}_3\text{H}_7-\text{O}-\text{C}=\text{O} \end{array}$	10.02 ± 0.02	9.47	0.55
n-Butyl acetate	$\begin{array}{c} \text{CH}_3 \\ \diagdown \\ \text{C}_4\text{H}_9-\text{O}-\text{C}=\text{O} \end{array}$	10.00 ± 0.03	9.44	0.56
Isobutyl acetate	$\begin{array}{c} \text{CH}_3 \\ \diagdown \\ \text{C}_4\text{H}_9-\text{O}-\text{C}=\text{O} \end{array}$	9.94 ± 0.03	9.36	0.58
n-Pentyl acetate	$\begin{array}{c} \text{CH}_3 \\ \diagdown \\ \text{C}_5\text{H}_{11}-\text{O}-\text{C}=\text{O} \end{array}$	9.92 ± 0.02	9.40	0.52
Methyl butyrate	$\begin{array}{c} \text{C}_4\text{H}_9 \\ \diagdown \\ \text{CH}_3-\text{O}-\text{C}=\text{O} \end{array}$	9.87 ± 0.02	9.44	0.43
Ethyl valerate	$\begin{array}{c} \text{C}_5\text{H}_{11} \\ \diagdown \\ \text{C}_2\text{H}_5-\text{O}-\text{C}=\text{O} \end{array}$	9.67 ± 0.03	9.19	0.48
n-Butyl butyrate	$\begin{array}{c} \text{C}_4\text{H}_9 \\ \diagdown \\ \text{C}_4\text{H}_9-\text{O}-\text{C}=\text{O} \end{array}$	9.57 ± 0.03	9.10	0.47

Table VIII. Ionization potentials of esters and their halogen derivatives (eV)

Compound	Formula	I_p of the halogen derivative of the ester	I_p of the ester	Difference (ΔI_p)
Methyl monochloroacetate	$\begin{array}{l} \text{ClCH}_2 \\ \text{CH}_3-\text{O} \end{array} \text{C}=\text{O}$	10.35 ± 0.03	10.25	0.10
Methyl dichloroacetate	$\begin{array}{l} \text{Cl}_2\text{CH} \\ \text{CH}_3-\text{O} \end{array} \text{C}=\text{O}$	10.44 ± 0.03	10.25	0.19
Ethyl monochloroacetate	$\begin{array}{l} \text{ClCH}_2 \\ \text{C}_2\text{H}_5-\text{O} \end{array} \text{C}=\text{O}$	10.20 ± 0.03	10.08	0.12
Ethyl trichloroacetate	$\begin{array}{l} \text{Cl}_3\text{C} \\ \text{C}_2\text{H}_5-\text{O} \end{array} \text{C}=\text{O}$	10.44 ± 0.03	10.08	0.36
Ethyl monobromoacetate	$\begin{array}{l} \text{BrCH}_2 \\ \text{C}_2\text{H}_5-\text{O} \end{array} \text{C}=\text{O}$	10.13 ± 0.03	10.08	0.05

increases the electron density in the benzene ring. This viewpoint agrees with the magnitudes and directions of the dipole moments of the alkyl derivatives of benzene. Besides, he considers that the size of the decrease in the ionization potential depends considerably on the interaction of the alkyl groups with the positive hole formed in the benzene ring upon ionization of one of the π -electrons.

In order to investigate further the effect of alkyl groups on the value of the ionization energy, the ionization potentials of many alkyl derivatives of benzene have been measured by the photoionization method in a number of studies.^[11,16,58] The results of these studies are compiled in the summary table. In addition, Fig. 13 shows the relation of the change in the ionization potential to the number of hydrogen atoms replaced by methyl groups on the benzene ring. An examination of these data shows that, there is a regular decline in the ionization potentials as we increase the number of substituents. Here the ionization-potential difference between successive members of the series gradually decreases as we go to the higher members

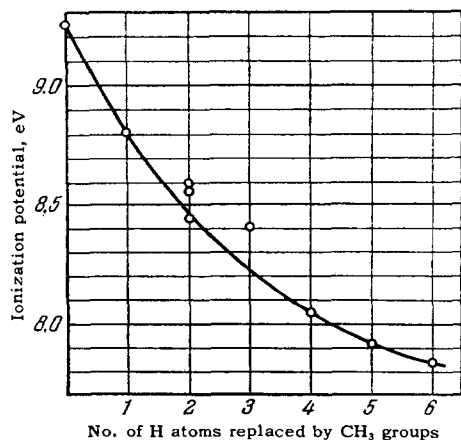


FIG. 13. Curve of the relation of the ionization potential to the structure of methyl derivatives of benzene.

of the series. Thus, it amounts to only 0.07 eV between pentamethyl- and hexamethylbenzene, while the ionization potential drops by 0.43 eV upon replacement of the first hydrogen atom. Evidently, the gradual decline in the differences between the successive members of the series results from the decrease in the effective charge of the positive hole as we go to the higher members of the series.

As was stated above, the variation of the energy of the ground state of the molecule and the corresponding ion can be traced from the stabilization energies. For this purpose, Table IX gives the stabilization energies of the molecules and the corresponding ions with respect to benzene. The data in the third and fourth columns are given as values per methyl group for convenience of examination. That is, they represent the contribution made by each methyl group to the stabilization energy of the whole molecule. For the first members of the series up to mesitylene, the stabilization energies S_{CH_3} of the molecules are taken from Price et al.^[16] There are as yet no reliable thermochemical data in the literature for the higher members of the series. On the basis of the constant contribution of each methyl group to the stabilization energy of the first members of the series, a contribution of 2.8 kcal/mole has been assumed for durene, pentamethylbenzene, and hexamethylbenzene, and the stabilization energies $S_{\text{CH}_3}^+$ of the corresponding ions have been calculated from the adiabatic ionization potentials.

An examination of these data indicates that the contribution of the methyl groups to the stabilization energy of the molecule is smaller by a factor of three or four than for the corresponding ion, and is practically invariant, whereas it decreases appreciably in the ion for the higher members of the series.

Aromatic amines. The aromatic amines have very diffuse absorption spectra. Hence one can determine precise values of their adiabatic ionization potentials only by the photoionization method.^[11,58,110] There are

Table IX. Stabilization energies of methyl derivatives of benzene (kcal/mole) and their ions with respect to benzene, calculated per methyl group

Compound	S_{CH_3}	$S_{CH_3}^+$	$S_{n+1}^+ - S_n^+$	Compound	S_{CH_3}	$S_{CH_3}^+$	$S_{n+1}^+ - S_n^+$
Toluene	2.9	12.6	12.6	Mesitylene	2.9	9.4	6.8
m-Xylene	2.67	10.6	8.6	Durene	2.8	9.5	9.8
o-Xylene	2.88	10.8	8.9	Pentamethylbenzene	2.8	8.8	6.1
p-Xylene	2.8	12.0	11.4	Hexamethylbenzene	2.8	8.2	5.1

two viewpoints on the ionization mechanism of the aromatic amines. According to one of them, the ionization process in the region of the first ionization potential involves the ejection of one of the π -electrons of the benzene ring.^[58,110] A number of authors adhere to the second viewpoint, according to which the ionization is due to the ejection of one of the unshared electrons of the nitrogen atom.^[111-114]

The photoionization-yield curves of the aromatic amines obtained in^[58,110] differ considerably from the analogous curves for other classes of compounds. As has been pointed out above for aniline (see Fig. 7), the ionization yield is very small near the ionization threshold, and gradually increases with increasing energy of the ionizing photons. The same type of curve is maintained throughout the other aromatic compounds containing the amino group. This indicates considerable changes in the interatomic distances in the molecules of aromatic amines upon ionization, which is more probably due to ejection of one of the electrons participating in a valence bond. Hence, we can assume that in ionization one of the π -electrons of the benzene ring is ejected. In confirmation of this viewpoint, ref-

erence^[110] has investigated the characteristics of the variation of different physical constants for a series of aromatic compounds (the positions of the first and second absorption bands λ_1 and λ_2 ; the dipole-moment differences $\Delta\mu$; and the exaltation of the molecular refraction for the sodium D-line (EMRD) as functions of the ionization potential. These data are given in Table X and in Fig. 14.

There is practically a linear relation between the ionization potentials and the positions of the first absorption bands of the various benzene derivatives. This indicates that the ionization and absorption involve the same electrons. The electrons that are common to all the cited compounds are the π -electrons of the benzene ring.

We can get further evidence of the ejection of π -electrons from the benzene ring upon ionization by comparing the ionization potentials of the amines. Thus, for example, the ionization potential of aniline is 7.69 eV, and that of m-toluidine is 7.50 eV, while their dissociation constants as bases are 4.0×10^{-10} and 5.5×10^{-10} , respectively. The latter fact indicates that the free electron-pair of the nitrogen atom is attracted

Table X. Some physical constants of benzene derivatives

Compound	λ_1 , Å; eV	λ_2 , Å; eV	λ_3 , Å; eV	$\Delta\mu$	EMRD	I_p ; eV
Benzene	2550 4.85	2020 6.15	1820 6.80	0 0.35	0.13	9.25
Toluene	2620 4.75	2050 6.05	1870 6.63	0.35	0.16	8.82
o-Xylene	2610 4.75				0.42	8.56
m-Xylene	2660 4.65				0.31	8.59
p-Xylene	2660 4.65				0.74	8.44
Mesitylene	2660 4.65				0.55	8.41
Phenol	2700 4.60	2130 5.83		0.7	0.26	8.52
Aniline	2850 4.35	2330 5.35	2000 6.20	0.9	0.86	7.69
m-Toluidine					1.13	7.50
Methylaniline	2880 4.30	2380 5.20	2000 6.20		1.16	7.35
Dimethylaniline	2970 4.17	2500 4.96	2000 6.20	1.5	1.58	7.14

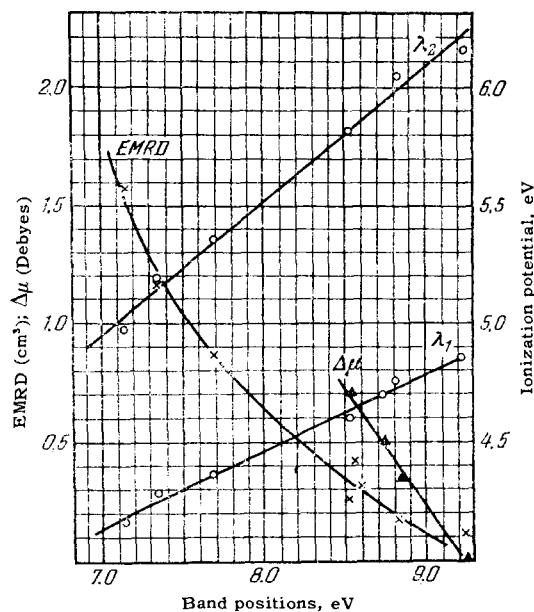
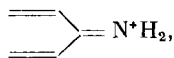


FIG. 14. Relation to the ionization potentials of the positions of: 1) the first, and 2) the second absorption bands, and 3) the exaltation of the molecular refraction, and 4) the dipole moment differences of aromatic amines and other benzene derivatives.

more weakly into the benzene ring for aniline than for *m*-toluidine. This contradicts the values of the ionization potentials, if we are to assume that one of the electrons of the nitrogen atom is ejected.

The considerably greater values of the exaltation of the molecular refraction and the dipole moments for the aromatic amines, as compared with the alkyl derivatives of benzene, indicate that the electrons of the free pair on the nitrogen are highly mobile and considerably conjugated with the benzene ring. When one of the π -electrons of the benzene ring is ejected and a positive hole is formed there, the displacement of the electrons of the free pair on the nitrogen can be so great that the bonds in the ring can rearrange to form a quinoid structure



which is the explanation of the color of the ions of organic amines in the theory of color.^[137]

We should note that the decrease in the ionization potentials in this series of compounds cannot be explained by a simple rise in the ground states of the molecules, as Scheibe^[115] assumes; he considers that in dyes the decrease in the ionization potential is due only to the change in the spacing between the ground and first excited states. A proof of this is the decrease in the energy spacing between the first and second excited levels, indicating a greater convergence of the electronic bands, and hence, a lowering of the ground states of the corresponding molecular ions.

Halogen derivatives of ethylene and benzene. Price and his associates^[116] have made a detailed study of the effect of halogen substituents on the electronic

spectra and ionization potentials of ethylene derivatives and aromatic compounds. On the basis of the precise ionization-potential values that they had obtained in this study, they showed that the effect of the substituents on the ionization potential, generally considered, is due to the induction effect, which mainly alters the binding of the electrons in the ground state of the molecule, and to the resonance-stabilization effect, which results from the interaction of the positive hole of the ion with the outer electrons of the substituent. They paid special attention to studying fluorinated compounds, since the effects for them are largest, and can have either sign.

The induction effect of fluorine atoms increases the first ionization potential of a number of compounds by several eV. Thus, for example, the ionization potential of methane is 12.99 eV, but that of perfluoromethane is 17.8 eV. Such a great increase in ionization potentials upon fluorination is also observed for other non-planar compounds, for which the induction effect dominates. For example, the ionization potential of ammonia is 10.154 eV, but that of NF_3 is 13.2 eV. In the latter case, the fluorine atoms exert a negative induction effect on the *p*-electrons of the nitrogen not involved in chemical bonding. As we remove the fluorine atom farther from the chromophoric group, the induction effect weakens considerably: thus, the ionization potential of methyl iodide is 9.54 eV, while that of F_3CI is 10.4 eV. An analogous phenomenon is observed in CH_3Br and CF_3Br , which have ionization potentials of 10.45 and 11.78 eV, respectively, and in toluene (8.82 eV) and α, α, α -trifluorotoluene (9.68 eV). As we decrease the number of fluorine atoms, the effect weakens proportionately, as α -fluorotoluene and α, α -difluorotoluene have ionization potentials of 9.12 and 9.45 eV, respectively.

In other cases, fluorination hardly alters the ionization potential, or conversely, decreases it. For example, the ionization potential of the methyl radical (9.84 eV) is reduced by complete fluorination to 9.5 eV. The CF_3 radical is planar. It exhibits a considerable overlap of the orbitals of the outer electrons of the fluorine and carbon. Hence, Price et al.^[116] explained the decrease in the ionization potential of CH_3 upon fluorination by the resonance-stabilization effect of the ion, which has a sign opposite to that of the induction effect, and which is superimposed on it. They studied this phenomenon in greater detail with the halogen derivatives of ethylene. They showed that stepwise fluorination of ethylene leads to a small decrease in the ionization potential of the double-bond electrons from 10.51 eV for ethylene to 10.12 eV for tetrafluoroethylene (Fig. 15). Here again, the two opposed effects almost completely balance. They found a more rapid decline in ionization potentials in the chlorinated and brominated ethylenes, and explained it by the dominant role of the resonance-stabilization effect over the induction effect.

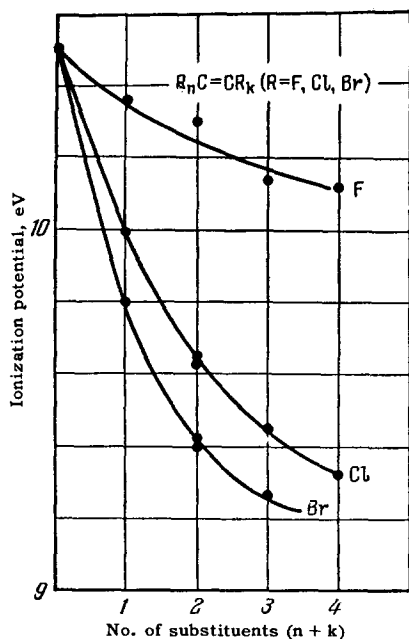


FIG. 15. Relations of the ionization potential to the structure of halogen derivatives of ethylene.

In contrast to ethylene, fluorination of benzene leads to an increase in the ionization potentials of the electrons of the ring, with the exception of monofluorobenzene and *p*-difluorobenzene, whose ionization potentials are 0.05 and 0.10 eV lower than that of benzene. Figure 16 shows the curve of the variation of the ionization potentials of the fluorinated benzenes as a function of the number of replaced hydrogen atoms. In contrast to ethylene, they established here also some appreciable changes in the ionization potentials depending on the positions of the substituents. Price explained these phenomena by the nature of the orbitals of the outer $(\pi_2)^2$ and $(\pi_3)^2$ electrons, which differ from the orbitals of ethylene. The nodal planes of the orbitals of benzene are normal to the plane of the ring, and pass through opposite carbon atoms or through the mid-points of opposite C—C bonds (Fig. 17). In the case of monofluoro- and *p*-difluorobenzene, the fluorine atoms are situated in the optimum positions for overlap of their *p*-electrons with the π -orbitals of the ring (Fig. 17, a). This results in maximum interaction, so that the conjugation effect somewhat exceeds the induction effect.

For substituents in the ortho-positions, the nodal plane passes through atoms 1 and 4, if the substituents are in positions 2, 3 or 5, 6 (Fig. 17, b). In this case the overlap of the wave functions is less, and we should expect smaller effects. However, the conjugation effects depend on overlap more strongly than the induction effect does, the value of the latter being approximately inversely proportional to the square of the distance to the "center of gravity" of the π -electrons. Thus, the latter effect may prove to be greater, and this is the reason why the ionization potential of

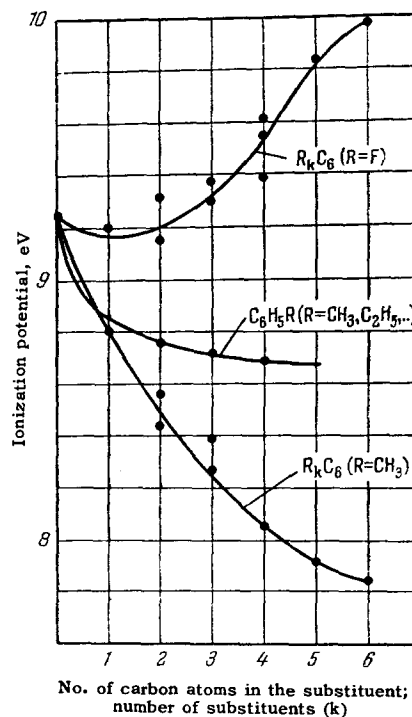


FIG. 16. Relations of the ionization potential to the structure of various benzene derivatives.

o-difluorobenzene (9.31 eV) is greater than that of benzene.

The presence of the separating nodal plane in *para*-substitution almost completely eliminates the mutual influence of substituents, and as we see from Table XI, the effects of the individual substituents are additive. An analogous phenomenon is observed with *o*-difluorobenzene, whose ionization potential is 0.06 eV higher than for benzene, and 1,2,4,5-tetrafluorobenzene, whose ionization potential is 0.14 eV higher than that of benzene. For any other tetrafluoro isomer, the ionization potential must be higher, since one of the fluorine atoms must be in a nodal plane. Consequently, it will exert no conjugation effect, although a weakened induction interaction will remain. In fact, the 1,2,3,4- and 1,2,3,5-isomers have larger ionization potentials: 9.61 and 9.55 eV, respectively. For the same reason, we should expect higher ionization potentials for pentafluorobenzene (9.85 eV) and hexafluorobenzene (9.97 eV).

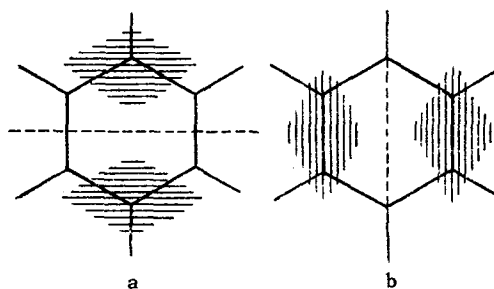


FIG. 17. Orbitals of benzene.

Table XI. Additivity of the variation of the ionization potentials upon *para*-substitution (Ionization-potential differences are given with respect to benzene, $I_p = 9.24$ eV)

X	Y	C_6H_5X	$p-C_6H_4X_2$	C_6H_5Y	$p-C_6H_4XY$
F	Δ F	9.20 -0.04	9.15 -0.09		
CH ₃	Δ CH ₃	8.82 -0.42	8.45 -0.79		
Cl	Δ Cl	9.07 -0.14	8.93 -0.31		
F	Δ CH ₃	9.20 -0.04	—	8.82 -0.42	8.78 -0.46
Cl	Δ CH ₃	9.07 -0.14	—	8.82 -0.42	8.69 -0.55
Br	Δ CH ₃	8.98 -0.26	—	8.82 -0.42	8.67 -0.57
I	Δ CH ₃	8.73 -0.51	—	8.82 -0.42	8.50 -0.74
F	Δ CF ₃	9.20 -0.04	—	9.68 0.44	9.69 0.45
F	Δ NH ₂	9.20 -0.04	— -1.54	7.70 -1.54	7.82 -1.42

Table XI, which is taken from [116], gives the ionization potentials of monosubstituted and *para*-disubstituted benzene derivatives. Even when the substituents differ, the rule of additive effects of *para*-substituents on the ionization potentials is quite well satisfied, and as a rule, the discrepancy does not exceed the experimental error (0.01–0.02 eV). Appreciable discrepancies have been observed only for *p*-fluoroaniline and *p*-iodotoluene. In general terms, this was explained by a proportional increase in the induction effect on the electrons in the ground state, owing to the considerably lower ionization potentials of aniline (7.70 eV) and toluene (8.82 eV), as compared with benzene (9.25 eV).

The ionization potentials of other classes of compounds are less well studied. However, the existing data also show regular changes that can be explained in analogous fashion. Thus, the very low ionization potentials of the condensed aromatic hydrocarbons (Fig. 18) may be due to the extension of the system of conjugated bonds.

8. IONIZATION POTENTIALS AND ELECTRONIC ABSORPTION SPECTRA OF ORGANIC COMPOUNDS

The shifting of absorption bands depends very strongly on the localization of the excited orbitals with respect to the molecular framework, and the estimation of the factors affecting the energy of the excited state is a difficult problem. [116] In most cases, a shift of the absorption bands to longer wavelengths corresponds in chromatological series to a decrease in the

ionization potentials. By analogy with the ionization potentials, the shift can be interpreted as resulting from a stronger stabilization of the excited states with respect to the ground state. As before, we denote as the stabilization energy the lowering of the corresponding level upon introduction of substituents due to the interaction of the electrons of the substituent and the chromophoric group.

For the near-ultraviolet absorption bands, the excited orbitals change by amounts insignificant in comparison with the distances between the substituent and the chromophoric group. Thus it would seem that the induction effect should exert the same action, in a first approximation, on both the ground and the excited

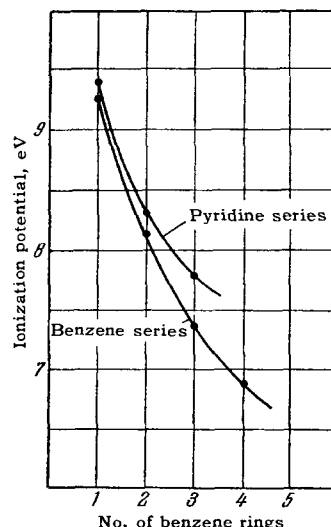


FIG. 18. Relation of the ionization potential to the number of rings in condensed aromatic compounds.

states. In other words, the induction effect should not contribute greatly to the shifts in the bands upon introduction of various substituents into the molecule. However, the polarization of the chromophoric group is greater in the excited state, since the binding of the excited electron to the molecular framework is weakened. This results in stronger polarization interactions between the substituent and the chromophoric group, and hence also to a greater lowering of the excited level than of the ground level upon introduction of substituents.

The degree of stabilization varies in parallel with the variation in the degree of excitation from small stabilization values for the low levels to large values for the high excitation levels; the limiting value corresponds to the ion. Thus, for example, the stabilization values for the ground state of toluene, its excited states corresponding to the 2700 and 1850 Å absorption bands, respectively, and the toluene ion, are approximately equal^[117] to 0.30, 3.2, 7.0, and 12.3 kcal/mole with respect to the corresponding levels of benzene. Analogous phenomena observed in the saturated hydrocarbons, the alkyl derivatives of ethylene, and other classes of compounds, can be explained in the same way.

As we should expect, the red shifts in the bands become more appreciable when the added substituent

forms a conjugated system with the original molecule, since here the stabilization effects of the excited states are enhanced owing to the great mobility of the π -electrons. This is graphically illustrated in Table XII,^[118] which gives the first absorption bands and the ionization potentials of certain classes of aromatic compounds.

When an atom or group of atoms having a large electron affinity and forming a conjugated system with a chromophoric group is joined to the latter, the changes in the ionization potentials and the shifts in the absorption bands can be opposed in direction. For example, the ionization potentials of benzophenone (9.45 eV), acetophenone (9.65 eV), and benzaldehyde (9.60 eV) are 0.2–0.4 eV higher than that of benzene (9.25 eV), while the first absorption bands are shifted by 600–700 Å to longer wavelengths with respect to the first absorption band of benzene. Perhaps in these compounds the first absorption bands are due to transitions of the p-electrons of oxygen to the π -orbitals of the benzene ring; however, the second absorption bands are also shifted considerably to the red. As was noted above, upon successive fluorination of ethylene there occurs a small gradual decrease in the ionization potentials, but at first the absorption bands undergo small red shifts, followed by a considerable blue shift for trifluoro- and tetrafluoroethylene.

Table XII. Absorption bands and ionization potentials of certain classes of aromatic compounds

Compound	λ_1 , Å; eV	λ_2 , Å; eV	λ_3 , Å; eV	I_p	$I_p - \lambda_1$	$I_p - \lambda_2$	$I_p - \lambda_3$
Benzene	2550 4.9	1980 6.25	1800 6.9	9.24	4.3	3.0	2,3
Naphthalene	3140 4.0	2750 4.5	2200 5.65	8.14	4.15	3.65	2.5
Anthracene	3800 3.26	—	2500 5.0	7.38	4.1	—	2.4
Naphthacene	4800 2.6	—	—	6.88	4.3	—	—
Pyridine	2500 5.0	1900 6.4	—	9.40	4.4	3.0	—
Quinoline	3110 4.0	2750 4.5	—	8.30	4.3	3.8	—
Acridine	3470 3.55	2520 4.9	—	7.78	4.23	2.9	—
Quinone	4200 3.36	3000 4.7	2500 5.65	9.68	6.3	5.0	4.0
Anthraquinone	4400 3.2	3230 4.4	—	9.34	6.1	5.0	—
α -Naphthylamine	3200 3.9	2400 5.2	—	7.30	3.4	2.1	—
β -Naphthylamine	3400 3.7	2800 4.4	2200 5.7	7.25	3.55	2,85	1,55
Benzaldehyde	3280 3.8	2800 4.45	2440 5.1	9.60	5.8	5.15	4.5
Acetophenone	3190 3.9	2780 4.45	2440 5.1	9.65	5,75	5.2	4.55
Benzophenone	3300 3.75	—	2520 4.9	9.45	5.7	—	4.55

Price^[116] has explained such anomalous changes in the ionization potentials and in the positions of the absorption bands by the action of the oppositely-directed negative induction effect and the conjugation effect. Since the lower and higher excited orbitals differ in localization, and the spatial laws of decline of these effects differ, the lower excited levels can be stabilized more with respect to the ground state of the molecule than the higher excited orbitals, including the ion.

The fact that the effects causing the variation of ionization potentials and the shifts in absorption bands in chromatological series are the same leads us to think that quantitative relations might exist between the ionization potentials and the positions of the absorption bands. The data of Table XII show that within a given class of compounds the differences between the ionization potentials and the corresponding absorption bands remain constant to an accuracy of 0.1–0.2 eV. With some caution, this empirical law can be used to estimate the adiabatic ionization potentials of the higher members of a series from the positions of the first absorption bands, provided that the ionization potentials of the first members of the same series have been reliably determined. However, as these data indicate, $I_p - \lambda_1$ differs considerably for different classes of compounds, by as much as 2 eV. Thus, for the series of linear polycyclic hydrocarbons from benzene to naphthacene, this difference is 4.1–4.3 eV, but for quinone and anthraquinone it is 6.1–6.3 eV.

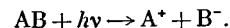
9. MASS-SPECTROMETRIC STUDY OF PHOTOIONIZATION PROCESSES

In studying the photoionization of molecular gases and vapors in order to get reliable values of the first ionization potentials of the molecules, the assumption has been made that only the process of elementary ionization according to the equation $AB + h\nu \rightarrow AB^+ + e$ occurs, while processes of dissociative photoionization are absent or require quanta of higher energy. Such a viewpoint has been justified in most cases, both by general energy considerations based on a knowledge of the ionization potentials of the radicals and the energies of the bonds in the molecules, and by experimental data from mass-spectrometric studies of ionization performed by the electron-impact method. The exceptions comprise molecules containing atoms or groups of atoms having high electron affinities.

In order to confirm these ideas directly, and also to study dissociative-photoionization processes in the region of the ionization continuum so as to get quantitative data on the appearance potentials and the cross-sections, one must make an analysis of the obtained products. The mass-spectrometric methods of analysis are the most suitable for this purpose, since they are highly sensitive and can be easily combined with the photoionization technique.

Terenin and Popov^[120] in 1932 were the first to

apply mass-spectrometric analysis to identify the products of photoionization of molecules. They established the decomposition of diatomic molecules into ions according to the following equation:



In recent years it has become possible to build mass-spectrometers in which photoionization is used instead of electron impact for generation of ions, based on the successful development of methods of studying photoionization.

Beginning in 1956, several papers have appeared in the literature on the study of photoionization applying the mass-spectrometric technique. A number of authors^[6,7,44,121,122] have independently reported the mass-spectrometric analysis of ion components obtained by photon bombardment using unresolved radiation. These studies showed that in the photon energy range up to 11.7 eV, the main photoionization process in most cases is elementary ionization. Fragment ions were either completely absent or their yields were quite small. The ion currents obtained at the mass-spectrometer collector in these first studies were high enough to make possible the replacement of the unresolved light by monochromatic light for detailed study of the elementary processes of interaction of high-energy photons with gases and vapors. It was also shown in^[7] that one can identify the products of ordinary photodissociation into neutral fragments by simultaneous irradiation of the ionization chamber of the mass-spectrometer with crossed beams of photons and electrons. The photon beam brought about photodissociation in the vapor being studied, while the low-energy electrons ionized the radicals that were formed.

A number of studies^[42,46,57,59,123,94,125] have been carried out in recent years on photoionization processes with successful application of a combination of a vacuum monochromator with a mass-spectrometer. The use of this technique has made it possible not only to get information on the types of ions formed, their appearance potentials, and the spectral dependence of the photoionization efficiency, but also in a number of cases to calculate such important energy characteristics as the dissociation energy of bonds in the molecules and the ions that are formed, heats of formation of the ions and radicals, and the ionization potentials of the radicals.

The first study of this type in a photon-energy range up to 11.7 eV was conducted by Inghram and his associates.^[42,44] Here they studied ethylamine, formaldehyde, acetone, methylethylketone, propylamine, propyl alcohol, and nitric oxide, and obtained the vertical and adiabatic ionization potentials. In addition, they identified the fragment ions and determined their appearance potentials and the spectral ionization-efficiency curves. The obtained results agreed satisfactorily with the data obtained previously by the photoionization and spectroscopic methods.

The next study by this group^[57] was concerned with the efficiency of photoionization of bromine, iodine, hydrogen iodide, and methyl iodide. They found in this study that for Br_2 and I_2 processes of the type $\text{AB} + h\nu \rightarrow \text{A}^+ + \text{B}^-$ require less energy than the process of elementary ionization. They also showed that the formation of pairs of ions is a preionization process, and they formulated criteria for establishment of preionization processes from the photoionization-efficiency curve.

Weissler and his group of associates^[46] have extended the range of energies of ionizing photons to 30 eV, and have obtained analogous data for argon, neon, helium, oxygen, nitrogen, nitrogen oxides, and carbon monoxide and dioxide.

In their most recent paper,^[34] Inghram and his associates have made a systematic study of the photoionization of the paraffins and the dissociation of the excited molecular ions in the photon-energy range up to 11.7 eV. Here they studied the effect of the thermal-energy supply of the molecule on the ionization-efficiency curves. They showed that the ionization-efficiency curves of the fragment ions are appreciably shifted to lower energies as the temperature of the mass-spectrometer chamber is increased from 300° to 415°K. They studied in detail the problem of the decomposition of metastable ions. They compared the experimental results with the conclusions from the statistical theory of dissociation kinetics. This theory is widely used in interpreting mass spectra. The agreement of this theory with the obtained results was quite unsatisfactory, which they explained by the defects of the theory.

Other authors^[59,125] have studied by an analogous method the methyl derivatives of benzene, aromatic amines, and hydrazine and its alkyl derivatives (Figs. 19–20).

I cannot even discuss briefly within the limits of

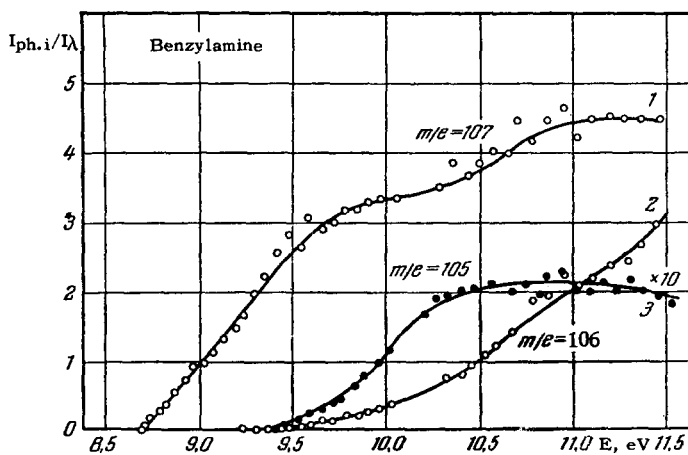


FIG. 19. Spectral-dependence curves of the photoionization efficiency of benzylamine. 1—Molecular ion; 2—ion minus one hydrogen atom; 3—ion minus two hydrogen atoms.

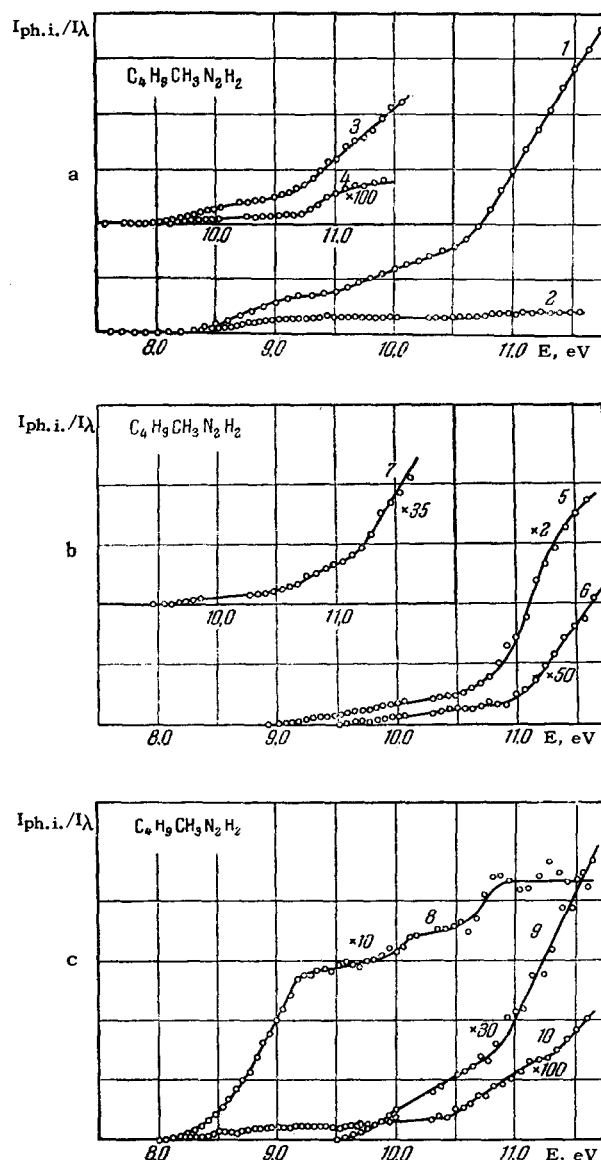


FIG. 20. Spectral-dependence curves of the photoionization efficiency of n-butylmethylhydrazine. 1—total ionization; 2—molecular ion, $M/e = 102$; 3— $M/e = 59$; etc.

this review all these studies in which extensive and valuable material has been obtained. In order to acquaint the reader briefly with the quantitative data of these studies, tables are given below of the appearance potentials, ionization processes, and other energy constants, as well as some typical ionization-efficiency curves for certain of the compounds studied (Tables XIII–XVI).

10. KINETIC-ENERGY DISTRIBUTION OF ELECTRONS IN PHOTOIONIZATION OF AROMATIC COMPOUNDS

The study of the effective photoionization cross-sections in absorption continua permits us to determine separately the amounts of absorbed energy spent

Table XIII. Ionization potentials and ionization processes in diatomic and triatomic molecules

Molecule and ionization process. Electronic state indicated in parentheses	Ionization potential, eV ^[46]	Molecule and ionization process. Electronic state indicated in parentheses	Ionization potential, eV ^[46]
$O_2(^3\Sigma_g^-) \rightarrow O_2^+(X^2\Pi_g)$	12.2±0.3	$CO_2 \rightarrow CO_2^+ \dots$	13.6±0.2
$\rightarrow O_2^+$	14.3±0.5	$\rightarrow CO_2^+ \dots$	14.9±0.2
$\rightarrow O_2^+(a^4\Pi_u)$	15.9±0.2	$\rightarrow CO_2^+ \dots$	17.0±0.2
$\rightarrow O_2^+(A^2\Pi_u)$	16.9±0.3	$\rightarrow CO_2^+ \dots$	18.8±0.3
$\rightarrow O_2^+(b^4\Sigma_g^-)$	18.8±0.4	$\rightarrow CO_2^+ \dots$	20.5±0.2
$\rightarrow O_2^+(?)$	21.2±0.4	$\rightarrow CO+O^+(^4S)$	19.2±0.3
$\rightarrow O^+(^4S)+O(^3P)$	18.8±0.4	$CO_2 \rightarrow CO+O^+$	20.3±0.2
$\rightarrow O^+(^2D)+O^-(^2P)$	20.7±0.4	$\rightarrow CO+O^+*(^2D)$	22.3±0.4
$\rightarrow O^+(^4S)+O^*(^1S)$	23.4±0.5	$\rightarrow CO+O^-(^2P)$	19.5±0.2
$N_2X^1\Sigma_g^+ \rightarrow N_2^+X^2\Sigma_g^-$	15.6±0.1	$\rightarrow CO^+ + O(^3P)$	20.5±0.2
$\rightarrow N_2^+(A^2\Pi_u)$	16.9±0.3	$\rightarrow CO^+ + O^*(^1D)$	23.3±0.0
$\rightarrow N_2^+(B^2\Sigma_u^+)$	18.8±0.4	$N_2O \rightarrow N_2O^+ \dots$	12.8±0.2
$\rightarrow N_2^+(?)$	20.7±0.4	$\rightarrow N_2O^+ \dots$	16.9±0.3
$\rightarrow N^+(^3P)+N(^4S)$	24.3±0.2	$\rightarrow N_2O^+ \dots$	18.8±0.4
or $N^+(^3P)+N^*(^2D)$		$\rightarrow N_2O^+ \dots$	20.7±0.3
$NO(X^2\Pi) \rightarrow NO^+(X^1\Sigma^+)$	9.2±0.1	$\rightarrow N_2(X^1\Sigma_g^+)+O^+(^4S)$	15.3±0.4
$\rightarrow NO^+(?)$	11.4±0.1	$\rightarrow N_2^+(X^2\Sigma_g^+)+O(^3P)$	17.4±0.2
$\rightarrow NO^+(?)$	12.8±0.2	$\rightarrow NO^+(X^1\Sigma^+)+N(^4S)$	15.3±0.4
$\rightarrow NO^+(\alpha)$	14.2±0.2	$\rightarrow NO^+(X^1\Sigma^+)+N^*(^2D)$	16.4±0.2
$\rightarrow NO^+(\beta)$	16.9±0.4	$\rightarrow NO(X^2\Pi)+N^+(^3P)$	20.0±0.3
$\rightarrow NO^+(\gamma)$	18.8±0.3	$NO_2 \rightarrow NO_2^+ \dots$	11.3±0.4
$\rightarrow NO^+(?)$	20.7±0.4	$\rightarrow NO_2^+ \dots$	12.5±0.1
$\rightarrow O^+(^4S)+N(^4S)$	19.5±0.2	$\rightarrow NO_2^+ \dots$	13.4±0.1
$\rightarrow O^+(^4S)+N^*(^2D)$	20.7±0.5	$\rightarrow NO_2^+ \dots$	15.3±0.4
$\rightarrow N^+(^3P)+O(^3P)$	21.8±0.4	$\rightarrow NO_2^+ \dots$	16.2±0.2
$CO(X^1\Sigma^+) \rightarrow CO^+(X^2\Sigma^+)$	13.9±0.2	$\rightarrow NO_2^+ \dots$	17.8±0.3
$\rightarrow CO^+(?)$	15.5±0.2	$\rightarrow NO_2^+ \dots$	20.0±0.3
$\rightarrow CO^+(A^2\Pi_u)$	16.6±0.3	$\rightarrow NO^+(X^1\Sigma^+)+O^-(^2P)$	11.3±0.4
$\rightarrow CO^+(?)$	18.4±0.3	$\rightarrow NO^+(X^1\Sigma^+)+O(^3P)$	12.5±0.1
$\rightarrow CO^+(B^2\Sigma^+)$	20.1±0.2	$\rightarrow NO^+(X^1\Sigma^+)+O^*(^1D)$	15.3±0.4
$\rightarrow CO^+(?)$	25.7±0.5	$\rightarrow NO^+(X^1\Sigma^+)+O^*(^1S)$	16.5±0.2
$\rightarrow C^+(^2P)+O^-(^2P)$	20.8±0.5	$\rightarrow NO^+(\alpha)+O(^3P)$	17.7±0.3
$\rightarrow C^+(^2P)+O(^3P)$	22.3±0.4	$\rightarrow NO^+(A^1\Pi)+O^-(^2P)$	20.3±0.3
$\rightarrow C^+(^2P)+O^*(^1D)$	24.8±0.5	$\rightarrow NO(X^2\Pi)+O^+(^4S)$	17.6±0.2
$\rightarrow C^+(^2P)+O^*(^1S)$	26.4±0.3	$\rightarrow NO(X^2\Pi)+O^+*(^1D)$	20.5±0.2

Table XIV. Ionization potentials and ionization processes of aromatic compounds*

Molecule and proposed photoionization process	Ionization potential	Ion current in relative units at $h\nu = 10.2$ eV
Benzene, $C_6H_6 \rightarrow C_6H_6^+$	9.17±0.08	100
$\rightarrow C_6H_6^{+*}$	10.3±0.1	
$\rightarrow C_6H_6^{+*}$	11.4±0.1	
Toluene, $C_6H_5CH_3 \rightarrow C_6H_5CH_3^+$	8.75±0.07	100
$\rightarrow C_6H_5CH_3^{+*}$	10.1±0.1	
p-Xylene, $C_6H_4(CH_3)_2 \rightarrow C_6H_4(CH_3)_2^+$	8.40±0.07	100
$\rightarrow C_6H_4(CH_3)_2^{+*}$	10.40±0.1	
Aniline, $C_6H_5NH_2 \rightarrow C_6H_5NH_2^+$	7.64±0.05	100
$\rightarrow C_6H_5NH_2^{+*}$	8.8±0.1	
$\rightarrow C_6H_5NH_2^{+*}$	10.1±0.1	
Methylaniline, $C_6H_5NHCH_3 \rightarrow C_7NH_9^+$	7.36±0.05	100
$\rightarrow C_7NH_9^{+*}$	8.6±0.1	
$\rightarrow C_7NH_9^{+*}$	10.0±0.1	
$\rightarrow C_7NH_8^+ + H$	11.0±0.1	
Dimethylaniline, $C_6H_5N(CH_3)_2 \rightarrow C_8NH_{11}^+$	7.10±0.05	100
$\rightarrow C_8NH_{11}^{+*}$	8.5±0.1	
$\rightarrow C_8NH_{11}^{+*}$	9.7±0.1	
$\rightarrow C_8NH_{10}^+ + H$	10.7±0.1	
Benzylamine, $C_6H_5CH_2NH_2 \rightarrow C_7NH_9^+$	8.66±0.05	100
$\rightarrow C_7NH_9^{+*}$	10.1±0.1	
$\rightarrow C_7NH_8^{+*} + H$	9.6±0.1	20
$\rightarrow C_7NH_7^+ + H_2$	9.9±0.1	6
$\rightarrow C_6H_5CH_2^+ + NH_2$		
$\{ C_6H_5CH_2 \rightarrow C_6H_5CH_2^+$		0.05
$\{ C_6H_5CH_2NH_2 \rightarrow C_6H_5 + CH_2NH_2$		
$\{ C_6H_5 \rightarrow C_6H_5^+$		0.08
$\{ C_6H_5CH_2NH_2 \rightarrow C_6H_5 + CH_2NH_2$		
$\{ CH_2NH_2 \rightarrow CH_2NH_2^+$		0.03
$\{ C_6H_5CH_2NH_2 \rightarrow C_6H_5CH_2 + NH_2$		
$\{ NH_2 \rightarrow NH_2^+$		0.01

*The ionization potentials of the molecular ions were determined from the appearance thresholds of the ions, and those of the fragment ions by the linear-extrapolation method; * denotes an excited state of the ion.^[59]

in ionization and in dissociation. However, the information obtained from these data on the distribution of the energy of the photon in excess of the adiabatic ionization potential of the molecule between the positive ion formed and the ejected electron cannot be considered to be satisfactory. In elementary photoionization, the efficiency curves are total curves obtained by superposition of the photoionization curves corresponding to each excited state of the ion. In most cases in the photoionization of complex organic molecules, the efficiency curves are smooth in nature. This prevents us from reliably identifying the positions of the excited states of the positive ions, and thus, from determining the fraction of the photon energy spent in exciting the ion.

In order to get reliable data on the distribution of the photon energy in excess of the ionization potential of the molecule, we must distinguish the ion-electron currents corresponding to ionization of the molecule to the different excited levels of the ion. This has been carried out in [47,48]; here the kinetic-energy distribution of the electrons in the photoionization of aromatic amines and methyl derivatives of benzene was studied by the stopping-field method in a cylindrical condenser. They obtained data from which they could establish the positions of the energy levels of the positive ions and estimate the probability of the ionization transition to each level as a function of the energy of the ionizing photons. Figures 21 and 22 show the energy-distribution curves of the electrons in the photo-

Table XV. Potentials and processes of ionization of hydrazine and its alkyl derivatives [125]. (Ion current in relative units is given for $h\nu = 11.2$ eV.)

Molecule and proposed photoionization process	Ionization potential, eV		Relative intensity	Heat of formation of ion, kcal/mole
	from appearance threshold of ions	linear extrapolation		
$N_2H_4 \rightarrow N_2H_4^+$	8.74 ± 0.06	—	100	224
$N_2H_4 \rightarrow N_2H_4^{+*}$	11.0 ± 0.1	—	—	—
$N_2H_4 \rightarrow N_2H_3^+ + H$	10.6 ± 0.1	11.1 ± 0.1	10	226
$N_2H_4 \rightarrow N_2H_2^+ + H_2$	—	—	—	(277)
$N_2H_3CH_3 \rightarrow CN_2H_6^+$	8.00 ± 0.06	—	100	207
$\rightarrow CN_2H_6^{+*}$	11.1 ± 0.1	—	—	—
$N_2H_3CH_3 \rightarrow CN_2H_5^+ + H$	9.2 ± 0.1	9.8 ± 0.2	22	196
$\rightarrow CN_2H_5^{+*} + H$	10.9 ± 0.2	10.9 ± 0.2	—	—
$\rightarrow CN_2H_4^+ + H_2$	9.4 ± 0.1	9.8 ± 0.1	7.5	249
$\rightarrow CN_2H_4^{+*} + H_2$	11.2 ± 0.1	11.2 ± 0.1	—	—
$\rightarrow CN_2H_3^+ + H_2 + H$	9.2 ± 0.2	11.4 ± 0.2	0.6	233
$\rightarrow N_2H_3^+ + CH_3$	9.5 ± 0.1	10.4 ± 0.1	0.6	228
$\rightarrow CH_3NH_2^+ + NH$	11.3 ± 0.1	11.3 ± 0.1	—	206
$H_2N_2(CH_3)_2 \rightarrow C_2N_2H_6^+$	7.69 ± 0.05	—	100	197
$\rightarrow C_2N_2H_6^{+*}$	10.6 ± 0.1	—	—	—
$\rightarrow C_2N_2H_5^{+*}$	11.2 ± 0.1	—	—	—
$\rightarrow C_2N_2H_7^+ + H$	8.7 ± 0.2	9.9 ± 0.1	10	196
$\rightarrow C_2N_2H_7^{+*} + H$	11.0 ± 0.2	11.0 ± 0.2	—	—
$\rightarrow C_2N_2H_6^+ + H_2$	9.5 ± 0.1	9.8 ± 0.1	3.5	246
$\rightarrow C_2N_2H_6^{+*} + H_2$	11.4 ± 0.2	11.4 ± 0.2	—	—
$\rightarrow CN_2H_5^+ + CH_3$	8.4 ± 0.1	8.7 ± 0.2	30	188
$\rightarrow CN_2H_5^{+*} + CH_3$	8.9 ± 0.1	8.9 ± 0.1	—	—
$\rightarrow C_2NH_7^+ + NH$	11.2 ± 0.2	11.2 ± 0.2	—	201
$\rightarrow C_2NH_6^+ + NH_2$	9.0 ± 0.2	9.8 ± 0.1	2.5	205
$\rightarrow C_2NH_6^{+*} + NH_2$	11.2 ± 0.2	11.2 ± 0.2	—	—
$\rightarrow N_2H_2^+ + C_2H_6$	8.6 ± 0.1	11.1 ± 0.1	0.1	289
$H_2N_2(C_2H_5)_2 \rightarrow C_4N_2H_{12}^+$	7.59 ± 0.05	—	100	184
$\rightarrow C_4N_2H_{11}^+ + H$	8.9 ± 0.1	9.4 ± 0.1	1.5	185
$\rightarrow C_4N_2H_{11}^{+*} + H$	11.1 ± 0.1	11.25 ± 0.1	—	—
$\rightarrow C_4N_2H_{10}^+ + H_2$	8.3 ± 0.2	9.2 ± 0.2	1.7	221
$\rightarrow C_4NH_{11}^+ + NH$	11.2 ± 0.1	—	2	191
$\rightarrow C_3N_2H_9^+ + CH_3$	8.0 ± 0.1	8.5 ± 0.2	120	195
$H_2N_2CH_2C_4H_9 \rightarrow C_5N_2H_{14}^+$	7.62 ± 0.05	—	100	180
$\rightarrow C_5N_2H_{14}^{+*}$	10.6 ± 0.1	—	—	—
$\rightarrow C_5N_2H_{13}^+ + H$	8.0 ± 0.3	8.2 ± 0.2	1	141
$\rightarrow C_5N_2H_{13}^{+*} + H$	10.4 ± 0.1	10.4 ± 0.1	—	—
$\rightarrow C_5N_2H_{12}^+ + H_2$	11.3 ± 0.1	11.3 ± 0.1	—	—
$\rightarrow C_5N_2H_{12}^{+*} + H_2$	8.0 ± 0.2	8.4 ± 0.1	1.6	200
$\rightarrow C_5N_2H_{11}^+ + CH_3$	10.6 ± 0.1	10.6 ± 0.1	—	—
$\rightarrow C_4N_2H_{11}^+ + CH_3$	8.0 ± 0.1	8.36 ± 0.06	115	164
$\rightarrow C_4N_2H_{11}^{+*} + CH_3$	9.6 ± 0.2	9.8 ± 0.2	—	—
$\rightarrow C_5NH_{13}^+ + NH$	10.5 ± 0.1	10.6 ± 0.1	—	171
$\rightarrow C_5NH_{12}^+ + NH_2$	9.0 ± 0.1	9.0 ± 0.1	0.7	136
$\rightarrow C_4N_2H_{11}^+ + CH_3$	—	—	3	—
$\rightarrow C_2N_2H_7^+ + C_3H_7$	9.1 ± 0.1	9.5 ± 0.1	110	196
$\rightarrow C_2N_2H_6^+ + C_3H_8$	9.5 ± 0.1	—	3	243
$\rightarrow CN_2H_5^+ + C_4H_9$	9.0 ± 0.1	9.1 ± 0.1	65	195
$\rightarrow CN_2H_5^{+*} + C_4H_9$	9.6 ± 0.1	9.6 ± 0.1	1	248
$\rightarrow N_2H_2^+ + n-C_4H_{11}$	9.5 ± 0.2	10.4 ± 0.1	1.5	274

Table XVI. Ion yield in photoionization of saturated hydrocarbons ($h\nu = 11.25$ eV, $T = 300^\circ\text{K}$) and appearance potentials of the fragment ions^[94]

Molecule, mass number in parentheses	Mass number of ion	Normalized ion yield	Mass number of metastable ion	Normalized yield of metastable ions	Appearance potential (eV) (linear extrapolation)
Ethane (30)	30	1.00	—	—	
	44	1.00	—	—	
Propane (44)	44	1.00	—	—	
	58	0.63	—	—	
n-Butane (58)	43	0.20	31.9	0.020	
	42	0.13	30.4	0.017	
Isobutane (58)	58	0.21	—	—	
	43	0.11	31.9	0.005	11.15±0.01
	42	0.68	30.4	0.006	10.89±0.01
n-Pentane (72)	72	0.43	—	—	
	57	0.041	45.1	0.0004	10.95±0.04
	56	0.031	43.6	0.001	10.84±0.01
	43	0.064	25.7	0.0004	11.04±0.03
Isopentane (72)	42	0.42	24.5	0.015	10.89±0.01
	72	0.24	—	—	
	57	0.066	45.1	0.0001	10.97±0.04
	56	0.20	43.6	0.008	10.68±0.01
Neopentane (72)	43	0.017	25.7	0.0001	11.14±0.02
	42	0.47	24.5	0.0025	10.74±0.01
	72	0.0006	—	—	
	57	0.86	45.1	0.0001	10.55±0.01
n-Hexane (86)	56	0.14	43.6	0.0001	10.37±0.01
	43	0.0006	25.7	0.002	
	42	0.0006	24.5	0.002	
	86	0.43	—	—	
2-Methylpentane (86)	71	0.015	58.6	0.002	10.89±0.05
	70	0.005	57.0	—	10.85±0.03
	57	0.14	37.8	0.003	10.86±0.04
	56	0.32	36.5	0.017	10.82±0.01
	43	0.006	21.5	0.001	11.14±0.03
	42	0.057	20.5	0.001	10.95±0.02
	86	0.25	—	—	
3-Methylpentane (86)	71	0.20	58.6	0.002	10.73±0.05
	70	0.13	57.0	—	10.67±0.01
	57	0.14	37.8	0.017	10.59±0.01
	56	0.092	36.5	0.008	10.54±0.01
	43	0.002	20.5	0.008	
	42	0.16	20.5	0.008	10.86±0.01
	86	0.19	—	—	
2,3-Dimethylbutane (86)	71	0.013	58.6	0.006	10.75±0.05
	70	0.013	57.0	—	10.63±0.03
	57	0.074	37.8	0.006	10.78±0.04
	56	0.70	36.5	0.012	10.49±0.01
	43	0.013	21.5	0.04	
	42	0.013	20.5	0.04	
	86	0.25	—	—	
2,2-Dimethylbutane (86)	71	0.18	58.6	0.026	10.58±0.05
	70	0.013	57.0	0.004	10.47±0.02
	57	0.0013	37.8	0.004	
	56	0.0013	36.5	0.004	
	43	0.003	21.5	0.04	11.24±0.04
	42	0.52	20.5	0.005	10.59±0.01
	86	0.005	—	—	
n-Heptane (100)	71	0.28	58.6	0.0005	10.47±0.03
	70	0.040	57.0	—	10.26±0.01
	57	0.23	37.8	0.0005	10.49±0.01
	56	0.45	36.5	0.0005	10.19±0.005
	43	0.009	21.5	0.027	
	42	0.009	20.5	0.027	
	100	0.50	—	—	
n-Heptane (100)	85	0.008	72.3	0.0015	10.79±0.06
	84	0.0026	70.6	0.005	10.87±0.02
	71	0.14	50.4	0.0025	10.80±0.05
	70	0.19	49.0	0.012	10.81±0.01
	57	0.024	32.5	0.0025	10.95±0.04
	56	0.10	31.4	0.005	10.87±0.01

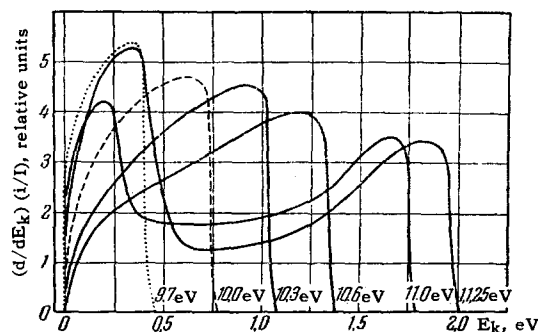


FIG. 21. The kinetic-energy distribution of the electrons in the photoionization of benzene. The curves are referred to a particular light-flux intensity.

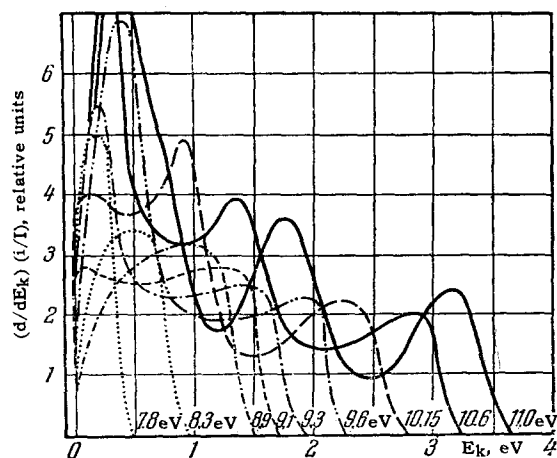


FIG. 22. The kinetic-energy distribution of the electrons in the photoionization of methylaniline. The curves are referred to a particular light-flux intensity.

ionization of benzene and methylaniline. The curves were obtained by graphical differentiation of the corresponding voltammetric curves, and were all referred to the same number of incident photons. Each curve in these diagrams corresponds to the particular value of the energy of the ionizing photons indicated near the horizontal (electron kinetic-energy) axis. When the difference between the energy of the ionizing photons and the ionization potential of the molecule of the substance being studied is small, these curves exhibit only

a single maximum, which shifts to higher kinetic energies as the energy quanta increase. With further increase in the photon energy, new maxima appear in the region of low electron energies, and these also shift to higher energies with increasing photon energy. For benzene, one observes the appearance of the first group of slow electrons when the photon energy exceeds the ionization potential by 1.5 ± 0.1 eV. For aniline, methylaniline, and dimethylaniline, an analogous group of electrons appears at an excess photon energy of 1, 1.2, and 1.1 eV, respectively. With further increase in photon energy, the latter three compounds exhibit a third group of electrons at photon energies exceeding the ionization potential by 2.4, 2.3, and 2.2 eV, respectively. Dimethylaniline exhibits a fourth group of electrons in the studied spectral range (6–11.7 eV) when the quantum energy exceeds the ionization potential by 2.8 eV.

The appearance of groups of slow electrons upon increase in the photon energy indicates the dissipation of a fraction of the photon energy within the absorbing system. Since it has been shown by direct experiments in [47] that the kinetic energies of the positive ions formed in photoionization are less than 0.1 eV, and no processes of dissociative ionization were detected in [59], the losses of the excess photon energy were ascribed to the excitation of the molecular ions to higher energy levels. Such an excitation of the ion might come about in two ways: by ejection of electrons from the deeper levels of the molecule, or by ejection of the least firmly bound electron with simultaneous transfer of a second electron to an excited level of the ion. Taking into account the data presented above, the energy equation can be written in the form

$$h\nu = I_p + E_{\text{excit}} + E_k,$$

where E_{excit} is the excitation energy of the ion, and E_k is the kinetic energy of the electron. If we know I_p , E_k , and $h\nu$, we can determine from this equation the positions of the energy levels of the molecular positive ions.

Some positions of excited levels of ions with respect to the ground state of the ion, as determined in this way, are given in Table XVII, together with the values of the first ionization potentials and the posi-

Table XVII

Compound	Ionization potential	Position of first level of ion	λ_1 , eV	λ_2 , eV	$\lambda_2 - \lambda_1$, eV
Benzene	9.25	1.5 ± 0.1	4.85	6.15	1.3
Toluene	8.82	1.3 ± 0.2	4.75	6.05	1.3
o-Xylene	8.56	1.3 ± 0.2	4.75		
m-Xylene	8.59	1.3 ± 0.2	4.65		
p-Xylene	8.44	1.3 ± 0.2	4.65		
Mesitylene	8.41	1.3 ± 0.2	4.65		
Durene	8.05	1.3 ± 0.2			
Aniline	7.69	1.2 ± 0.1	4.35	5.35	1.0
Methylaniline	7.34	1.1 ± 0.1	4.30	5.20	0.9
Dimethylaniline	7.14	1.0 ± 0.1	4.17	4.96	0.8

tions of the maxima of the first and second absorption bands. As we see from Table XVII, the spacing from the ground state to the first excited level of the ion agrees rather well with the difference in the energy quanta corresponding to the second and first absorption bands. If we assume that the first absorption band of benzene and its derivatives arises from the excitation of electrons from the uppermost level, while the second absorption band arises from excitation of electrons from a lower level,^[138] this comparison favors the first mechanism of excitation of the positive ion by ejection of the more firmly bound π -electrons of the benzene ring.

Several different energy spectra of electrons have been obtained in the study of the methyl derivatives of benzene. A characteristic peculiarity of them is the fact that when a group of slow electrons appears, the maximum of the fast-electron peak does not shift toward higher kinetic energies, but remains in place over a rather large range of photon energies (Fig. 23).

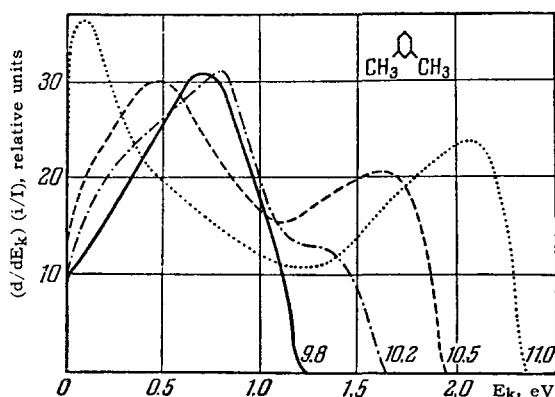


FIG. 23. The kinetic-energy distribution of the electrons in the photoionization of *m*-xylene. The curves are referred to a particular light-flux intensity.

This experimental fact has been explained by preionization processes proceeding from highly-excited levels of the molecule lying between the ground and first excited levels of the ion to the ground state of the ion. Here the absorption coefficients in the preionization bands should be considerably greater than for ordinary ionization transitions. For *m*-xylene, mesitylene, and durene, at photon energies exceeding the ionization potential by 2.6–2.3 eV, the appearance of a distinct group of electrons of zero energy has been observed. As before, this was explained by ionization transitions to an excited level of the ion.

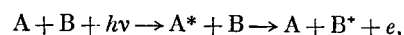
We can estimate the probability of photoionization transitions from the ground state of the molecule to various electronic levels of the ion by comparing the heights of the peaks on the energy-distribution curves of the photoionization electrons. A comparison of the peak heights shows that with increasing quantum energy, the contributions of the transitions to the lower

levels of the ion to the total photoionization yield decrease slightly. One can get more precise data along this line by comparing the areas under the corresponding peaks, but such an analysis has not yet been performed.

The study of the energy spectra of photoionization electrons from complex organic vapors is of direct interest in problems of solid-state physics as well. An appreciable dissipation of the energy of the absorbed photons has been found on studying the external photoeffect from polycrystalline layers of organic dyes. This is manifested in the fact that, with increasing photon energy, the predominating fraction of the electrons is emitted with exceedingly small energies.^[132,133] This was hypothetically explained, not by the dissipation of the kinetic energy of the photoelectrons during their movement to the surface of the layer, as occurs with a number of inorganic semiconductors, but by the excitation of the positive ions that are formed. In the most recent study along this line,^[255] a qualitative agreement was shown by the direct method of photoionization of the gaseous dye between the energy-distribution curves of the electrons upon photoionization of rhodamine 6G in the gas phase and in the external photoeffect from layers of the same dye. These data fully confirmed the previously-proposed mechanism of dissipation of the energy of the photons in excess of the photoelectric work function in the external photoeffect.

11. SENSITIZED PHOTOIONIZATION

Tanaka and Steacie^[126] obtained much larger photoionization currents upon irradiation of a gaseous mixture of nitric oxide and krypton with a resonance krypton lamp than upon irradiation of pure nitric oxide under the same conditions. This showed that a sensitized-photoionization process is taking place according to the mechanism:



where A is a gas atom, krypton in this case, A* is its excited state, and B is a molecule, NO in this case, having an ionization potential lower than the energy of the resonance level of the atom A. In essence this process is analogous to sensitized fluorescence, which has been studied in detail for a number of systems at present.^[127,128]

In a subsequent study, these same authors^[129] made a detailed investigation under various conditions of the ionization of nitric oxide ($I_p = 9.25$ eV) and acetone ($I_p = 9.69$ eV) by the resonance lines of krypton (10.0 and 10.6 eV). They likewise obtained the sensitized photoionization of the same vapors by argon (energy of resonance lines = 11.6 and 11.8 eV), and of anisole ($I_p = 8.20$ eV) by xenon (energy of resonance lines = 8.4 and 9.53 eV). The relation of the values of the photoionization currents in pure nitric oxide and in a

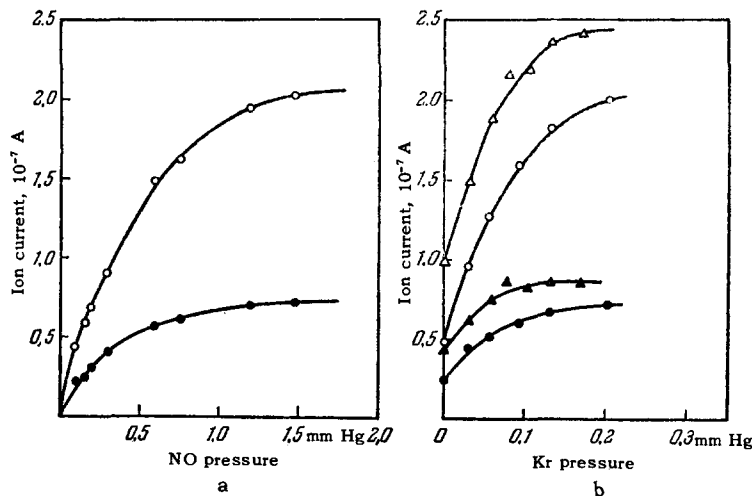


FIG. 24. Photoionization of (a) nitric oxide (with potential differences between electrodes of 22.5 V —●, and 45 V—○); and of (b) a nitric oxide-krypton mixture. ●—Potential difference 22.5 V, pressure 0.11 mm Hg; ▲—22.5 V, 0.29 mm Hg; ○—45 V, 0.11 mm Hg; △—45 V, 0.29 mm Hg.

nitric oxide-krypton mixture (Fig. 24) to the pressure was measured at various voltages across the electrodes of the photoionization cuvette. The results clearly show greater ion currents in the mixture than in pure nitric oxide. The curves of Fig. 24 were used to find the photoionization cross-section σ_1 . The obtained value $\sigma_1 = 1.31 \times 10^{-17} \text{ cm}^2$ differs considerably from the data obtained by Watanabe,^[52] who found a cross-section of $1 \times 10^{-18} \text{ cm}^2$ at 1300 Å, and $6 \times 10^{-18} \text{ cm}^2$ at 1100 Å. The reason for such a considerable discrepancy has not been elucidated.

Figure 25 shows the variation in the ion current in the photoionization of pure nitric oxide by the radiation from a krypton resonance lamp due to the addition of hydrogen, deuterium, or helium. Increase in the pressure of the added gases decreases the ion current. The greatest decreases are observed for hydrogen, and the least for helium. The decrease in the ion current has

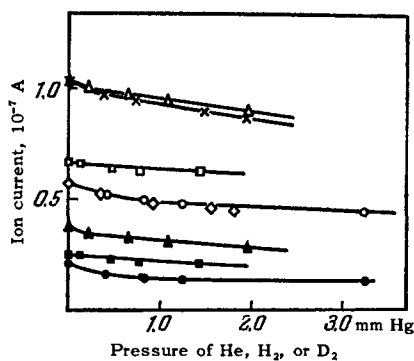


FIG. 25. Quenching of the photoionization of nitric oxide by helium, hydrogen, and deuterium.

NO pressure, mm Hg	Gas	Potential, V	NO pressure, mm Hg	Gas	Potential, V
△—0.36	D ₂	45	○—0.15	D ₂	45
×—0.36	H ₂	45	▲—0.36	D ₂	22.5
□—0.20	He	45	■—0.20	He	22.5
◇—0.15	H ₂	45	●—0.15	D ₂	22.5

been explained by an increase in the probability of recombination processes between the positive ions and the electrons.

Figure 26 gives curves for the ion current in mixtures of NO + Kr + He (or H₂ or D₂) as a function of the pressure of the He or H₂ or D₂. In the lower curves, for which the NO pressure is small, processes of deactivation of excited krypton atoms by hydrogen or deuterium atoms play the major role. Here H₂ deactivates Kr* more effectively than D₂ does; an analogous phenomenon has been observed in the deactivation of Cd* and K*.^[130,131]

The character of the curves at high pressures is explained by the competition of two opposite effects: the deactivation of excited krypton atoms, which decreases the ion current, and the broadening of the

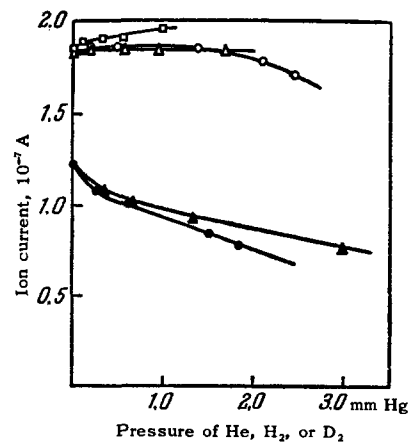
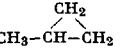
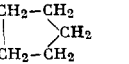
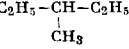
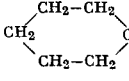


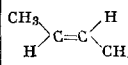
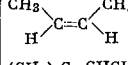
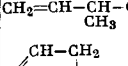
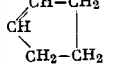
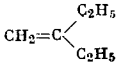
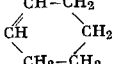
FIG. 26. Quenching of the krypton-sensitized photoionization of nitric oxide by helium, hydrogen, and deuterium.

Quenching gas	NO pressure, mm Hg	Kr pressure, mm Hg
□—He	0.36	0.090
○—H ₂	0.36	0.090
△—D ₂	0.36	0.086
●—H ₂	0.085	0.090
▲—D ₂	0.085	0.090

Table XVIII

Compound	Formula	Ionization potential eV			
		Photoionization	Spectroscopy	Electron impact	Semi-empirical calculation
Organic compounds					
1. Methane*	CH ₄	12.99±0.0411 12.8±0.278		13.1171 13.16179 13.082 13.04172	14.0699
2. Ethane	CH ₃ -CH ₃	11.65±0.0311		11.6173 11.7662	12.0499
3. Propane	CH ₃ -CH ₂ -CH ₃	11.08±0.0311		11.3175 11.2162	11.1299 11.2299
4. Cyclopropane	(CH ₂) ₃	10.06±0.0316 10.09±0.0211		10.23176	11.7666
5. n-Butane	CH ₃ (CH ₂) ₂ CH ₃	10.63±0.0311		10.34177 10.8082	10.9768
6. Isobutane	(CH ₃) ₂ CH-CH ₃	10.55±0.0516		10.34174 10.40177	10.6366 10.7366
7. Methylcyclopropane				9.8866	10.9866
8. n-Pentane	CH ₃ -(CH ₂) ₃ CH ₃	10.33±0.0516		10.5562 10.5172	10.6366 10.5699
9. 2-Methylbutane	(CH ₃) ₂ CH-C ₂ H ₅	10.32±0.253		10.1172	10.4366
10. Cyclopentane		10.51±0.0316 10.95±0.05253			
11. Neopentane	(CH ₃) ₄ C	10.37±0.0716		10.29178	10.2166
12. n-Hexane	CH ₃ (CH ₂) ₄ CH ₃	10.17±0.0516		10.54179 10.4362 10.4160 10.1143	10.5266 10.4160 10.4299
13. 2-Methylpentane	(CH ₃) ₂ CH-C ₃ H ₇	10.09±0.0516		10.1172	
14. 3-Methylpentane		10.06±0.0516		9.8172	
15. 2,3-Dimethylbutane	(CH ₃) ₂ CH-CH(CH ₃) ₂	10.00±0.0516		10.1172	10.2166
16. 2,2-Dimethylbutane	(CH ₃) ₃ C-C ₂ H ₅	10.04±0.0516		10.19178	10.1166
17. Cyclohexane		9.88±0.0211	9.286	9.24179 10.3180	10.2166
18. n-Heptane	CH ₃ (CH ₂) ₅ CH ₃	10.06±0.0516		10.3562 10.00172	10.4466 10.3399
19. 2,2,3-Trimethylbutane	(CH ₃) ₃ C-CH(CH ₃) ₂			10.09178	9.9466
20. Methylcyclohexane	CH ₃ -C ₆ H ₁₁	9.86±0.0216			
21. n-Octane	CH ₃ (CH ₂) ₆ CH ₃			10.2462	10.3866 10.2799
22. 2,2,4-Trimethylpentane	(CH ₃) ₃ C-CH ₂ -CH(CH ₃) ₂	9.84±0.0516			
23. 2,2,3,3-Tetramethylbutane	(CH ₃) ₃ C-C(CH ₃) ₃			9.78178	9.7466

*CD₄-13.21[62]

Compound	Formula	Ionization potential, eV			
		Photoionization	Spectroscopy	Electron impact	Semi-empirical calculation
24. n-Nonane	CH ₃ (CH ₂) ₇ CH ₃			10.2162	10.2299
25. n-Decane	CH ₃ (CH ₂) ₈ CH ₃			10.1962	10.3366 10.1999
26. Ethylene*	CH ₂ =CH ₂	10.516±0.0411 10.47±0.02134	10.5015 10.51436	10.6262 10.5633	
27. Propylene	CH ₂ =CH-CH ₃	9.73±0.0411 9.73±0.0291	9.7015 9.736	9.8462 9.8033	
28. 1-Butene	CH ₂ =CH-CH ₂ -CH ₃	9.61±0.0294 9.58±0.0111		9.65214 9.7662	9.7066
29. Isobutylene	(CH ₃) ₂ C=CH ₂	9.23±0.0216		9.3562	9.2866
30. Trans-2-butene		9.13±0.0116	9.236	9.2762 9.2933	9.2866
31. Cis-2-butene		9.13±0.0116		9.2962 9.3233	9.2866
32. Trimethylethylene	(CH ₃) ₂ C=CHCH ₃	8.68±0.0116	8.7536	8.8562	8.8166
33. Tetramethylethylene	(CH ₃) ₂ C=C(CH ₃) ₂	8.30±0.0116	8.336		
34. 1-Pentene	CH ₂ =CH(CH ₂) ₂ CH ₃	9.50±0.0294 9.50±0.0216		9.6662	9.6766
35. 3-Methyl-1-butene		9.51±0.0216			
36. Cyclopentene				10.2179	
37. 1-Hexene	CH ₂ =CH(CH ₂) ₃ CH ₃	9.45±0.0294 9.46±0.0216		9.5962	9.5666
38. Trans-2-hexene	CH ₃ -CH=CH-C ₃ H ₇			9.1662	
39. Trans-3-hexene	C ₂ H ₅ -CH=CH-C ₂ H ₅			9.1262	9.1166
40. 2-Ethyl-1-butene				9.2162	
41. Cyclohexene		8.945±0.0111	9.211	9.2462	9.1666
42. 1-Heptene	CH ₂ =CH(CH ₂) ₄ CH ₃				9.5462
43. 1-Octene	CH ₂ =CH(CH ₂) ₅ CH ₃				9.5262
44. 2-Octene	CH ₃ -CH=CH(CH ₂) ₄ CH ₃				9.1162
45. 1-Decene	CH ₂ =CH(CH ₂) ₇ CH ₃				9.5162
46. Allene	CH ₂ =C=CH ₂		10.19117	10.0216	
47. 1,3-Butadiene	CH ₂ =CH-CH=CH ₂	9.07±0.0111	9.06337	9.24179	

*C₂D₄-10.46[36]

Table XVIII (cont'd)

Compound	Formula	Ionization potential, eV			
		Photoionization	Spectroscopy	Electron impact	Semi-empirical calculation
48. 2-Methyl-1,3-butadiene	<chem>CH2=CH=CH=CH2</chem> <chem>CH3</chem>	8.85±0.0116	8.8637	9.08179	8.866 8.566
49. Cyclopentadiene	<chem>C1=CC=CC1</chem>		8.5837 8.62144	8.733	9.166 8.7566
50. 2,3-dimethyl-1,3-butadiene	<chem>CH2=C(CH3)-C(CH3)=CH2</chem>	8.72±0.0116	8.3015 8.6714		8.666 8.366
51. 1,3,5-Hexatriene	<chem>C6H8</chem>		8.2639		8.05; 8.566
52. Cyclohexadiene	<chem>C6H8</chem>		8.4037		8.42; 8.1266
53. 1,3,5,7-Octatetraene	<chem>C8H10</chem>		7.839		8.23; 7.6666
54. Cyclooctatetraene	<chem>C8H8</chem>			8.63215	
55. Acetylene	<chem>HC#CH</chem>	11.41±0.0111 11.25±0.0593	11.4195	11.4362 11.4233	
56. Methylacetylene	<chem>CH3-C#CH</chem>	10.36±0.0111* 10.36±0.01136*	10.36135* 11.2597 11.2590145 11.2417145	10.3988*	
57. Ethylacetylene	<chem>CH3-CH2-C#CH</chem>	10.18±0.01135* 10.18±0.0111*		10.34219	
58. Dimethylacetylene	<chem>CH3-C#C-CH3</chem>		9.85117* 11.45145**	9.85219*	
59. Propylacetylene	<chem>CH3-CH2-CH2-C#CH</chem>			10.39219	
60. Isopropylacetylene	<chem>(CH3)2CH-C#CH</chem>			10.35219	
61. Divinylacetylene	<chem>CH2=CH-C#C-CH=CH2</chem>		10.539		
62. Diacetylene	<chem>CH#C-C#CH</chem>		10.7397 10.741145	11.3219	
63. Methanol	<chem>CH3-OH</chem>	10.85±0.0211 10.52±0.03134	1	10.8833 10.95179	
64. Ethanol	<chem>CH3-CH2-OH</chem>	10.50±0.0552 10.50±0.0511 9.23136		10.797 10.60179	10.5466
65. n-Propyl alcohol	<chem>CH3-(CH2)2-OH</chem>	10.15117		10.46179	
66. Isopropyl alcohol	<chem>(CH3)2CH-OH</chem>	10.15±0.0511		10.46179 10.27221	
67. n-Butyl alcohol	<chem>CH3-(CH2)3-OH</chem>	10.1117		10.30221	
68. Isobutyl alcohol	<chem>(CH3)2CH-CH2-OH</chem>	10.1117		10.17221	
69. tert-Butyl alcohol	<chem>(CH3)3C-OH</chem>	9.7117		9.92221	
*These I _p values may refer to the formation of an allene-type ion. **Second ionization potential.					

Compound	Formula	Ionization potential, eV			
		Photoionization	Spectroscopy	Electron impact	Semi-empirical calculation
70. Dimethyl ether	<chem>(CH3)2O</chem>	10.00±0.0211		10.587	
71. Diethyl ether	<chem>(C2H5)2O</chem>	9.53±0.0211 9.55±0.03103		9.72179 10.297	9.7666
72. Di-n-propyl ether	<chem>(C3H7)2O</chem>	9.28±0.05103			
73. Di-n-butyl ether	<chem>(C4H9)2O</chem>	9.18±0.05103			
74. Ethylene oxide	<chem>C1CO1</chem>	10.565±0.0111	10.81224	11.2224	
75. Tetrahydrofuran	<chem>C1CCOC1</chem>	9.48±0.02103		10.1179	
76. 1,4-Dioxane	<chem>C1CCOCCO1</chem>	9.13±0.03253		9.52179	
77. Furan	<chem>C1C=CCO1</chem>	8.89±0.0111	9.01226 9.06226	9.0226	
78. Formaldehyde	<chem>CH2O</chem>	10.87±0.0111 10.90±0.0358	10.88101* 10.8397* 11.8148**	10.8225	
79. Formaldehyde dimer	<chem>(CH2O)2</chem>	10.51±0.0358			
80. Acetaldehyde	<chem>CH3-CHO</chem>	10.21±0.0111 10.20±0.0358	10.18148 10.18139 10.22538	10.28179	
81. Propionaldehyde	<chem>CH3-CH2-CHO</chem>	9.98±0.20153		10.06179	10.1166
82. Butyraldehyde	<chem>CH3-CH2-CH2-CHO</chem>	9.86±0.02253		10.01179	10.0866
83. Isovaleraldehyde	<chem>CH3-CH(CH3)-CH2-CHO</chem>	9.71±0.05253		9.92179	9.9966
84. Acrolein	<chem>CH2=CH-CHO</chem>	10.10±0.0111	10.057151* 11.241**	10.34179	
85. Crotonaldehyde	<chem>CH3-CH=CH-CHO</chem>	9.73±0.0111	10.1997		
86. Glyoxal	<chem>O=C-C(=O)H</chem>		10.4152*		
87. Acetone	<chem>CH3-CO-CH3</chem>	9.690±0.0152 9.71±0.0358	9.70511* 10.26150* 11.344**	10.187 9.92179	
*p-electrons of oxygen. **π-electrons.					

Table XVIII (cont'd)

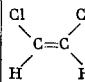
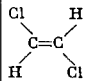
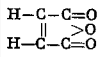
Compound	Formula	Ionization potential, eV				Compound	Formula	Ionization potential, eV			
		Photoionization	Spectroscopy	Electron impact	Semi-empirical calculation			Photoionization	Spectroscopy	Electron impact	Semi-empirical calculation
88. Methyl ethyl ketone	CH ₃ COC ₂ H ₅	9.54±0.0358 9.54±0.0252		9.76179	8.8466 9.7466	115. Formic acid	HCOOH	11.05±0.0111 11.05±0.0358	11.33259	11.54179	
89. Methyl propyl ketone	CH ₃ COC ₃ H ₇	9.47±0.0358 9.39±0.02258		9.59179	9.7266	116. Acetic acid	CH ₃ -COOH	10.35±0.0311 10.38±0.0358		10.70179	
90. Methyl butyl ketone	CH ₃ COC ₄ H ₉	9.44±0.0358		9.58179		117. Propionic acid	C ₂ H ₅ COOH	10.09±0.0211		10.47179	
91. Methyl n-octyl ketone	CH ₃ COC ₈ H ₁₇	9.40±0.0358				118. Butyric acid	C ₃ H ₇ COOH	10.16±0.05253		10.22179	
92. Diethyl ketone	C ₂ H ₅ COC ₂ H ₅	9.34±0.02103				119. Acrylic acid	CH ₂ =CHCOOH			10.90179	
93. Ethyl tert-butyl ketone	C ₂ H ₅ COC(CH ₃) ₃	8.98±0.02103				120. Methyl fluoride	CH ₃ F			12.7233	
94. Dipropyl ketone	C ₃ H ₇ COC ₃ H ₇	9.12±0.03102				121. Bromodifluoromethane	CHBrF ₂			12.1209	
95. n-Propyl n-butyl ketone	C ₃ H ₇ COC ₄ H ₉	9.10±0.05102				122. Chlorotrifluoromethane	CClF ₃			12.8206	
96. Diisobutyl ketone	(CH ₃) ₂ CHCH ₂ COCH ₂ CH(CH ₃) ₂	9.04±0.03102				123. Ethyl fluoride	C ₂ H ₅ F			12.00227	
97. Pinacolone	(CH ₃) ₂ CCOCH ₃	9.18±0.03102				124. Vinyl fluoride	H ₂ C=CHF	10.37±0.02116			
98. Pentamethylacetone	(CH ₃) ₂ CHCOC(CH ₃) ₃	8.82±0.02103				125. Difluoroethylene	H ₂ C=CF ₂	10.30±0.02116			
99. Pivalone	(CH ₃) ₃ CCOC(CH ₃) ₃	8.65±0.03102				126. Trifluoroethylene	HFC=CF ₂	10.14±0.02116			
100. Cyclopentanone	(CH ₂) ₄ CO	9.27±0.03102				127. Tetrafluoroethylene	F ₂ C=CF ₂	10.12±0.02116			
101. Cyclohexanone	(CH ₂) ₅ CO	9.14±0.03102				128. Methyl chloride	CH ₃ Cl	11.28±0.0111 11.1714	11.22153 11.1714	11.46179 11.3533	
102. Camphor	C ₁₀ H ₁₆ O	8.76±0.03102				129. Methylene dichloride	CH ₂ Cl ₂	11.35±0.0211		11.4228	
103. Ketene	H ₂ C=C=O		9.60117	9.4194		130. Chloroform	CHCl ₃	11.42±0.0311			
104. Diketene	CH ₂ =C(CH ₂) ₂ O=CO			9.4194		131. Carbon tetrachloride	CCl ₄	11.47±0.01		11.1229	
105. Methyl acetate	CH ₃ COOCH ₃	10.27±0.02253	10.2117			132. Ethyl chloride	CH ₃ -CH ₂ -Cl	10.97±0.0211	10.89153	11.18179	10.9666
106. Ethyl acetate	CH ₃ COOC ₂ H ₅	10.09±0.0211 10.08±0.02103		9.97179		133. n-Propyl chloride	CH ₃ -CH ₂ -CH ₂ -Cl	10.82±0.03253		10.7230 10.96179	10.7166 10.9966
107. n-Propyl acetate	CH ₃ COOC ₃ H ₇	10.02±0.02103				134. n-Butyl chloride	CH ₃ (CH ₂) ₃ -Cl	10.125±0.0111			
108. n-Butyl acetate	CH ₃ COOC ₄ H ₉	10.00±0.03103				135. tert-Butyl chloride	(CH ₃) ₃ C-Cl			10.2230	10.13; 10.7566
109. Isobutyl acetate	CH ₃ COOCH ₂ CH(CH ₃) ₂	9.94±0.03103				136. Vinyl chloride	CH ₂ =CHCl	9.995±0.01116 10.1096	9.95155	10.0155	
110. n-Pentyl acetate	CH ₃ COOC ₅ H ₁₁	9.92±0.02103				137. cis-Dichloroethylene		9.65±0.01116	9.6197 9.66155	9.66155	
111. Methyl butyrate	C ₃ H ₇ COOCH ₃	9.87±0.02103				138. trans-Dichloroethylene		9.63±0.03116	9.9197 9.96155	9.96155	
112. Ethyl valerate	C ₄ H ₉ COOC ₂ H ₅	9.67±0.03103				139. 1,1-Dichloroethylene	CH ₂ =CCl ₂	9.79±0.02116			
113. Butyl butyrate	C ₃ H ₇ COOC ₄ H ₉	9.57±0.03103									
114. Maleic anhydride			9.9117								

Table XVIII (cont'd)

Compound	Formula	Ionization potential, eV			
		Photoionization	Spectroscopy	Electron impact	Semi-empirical calculation
140. Trichloroethylene	$\text{Cl}_2\text{C}=\text{CHCl}$	$9.47 \pm 0.0411^{**}$ $9.45 \pm 0.0211^*$	9.79155*	9.94179	
141. Tetrachloroethylene	$\text{Cl}_2\text{C}=\text{CCl}_2$	$9.32 \pm 0.0211^{**}$	9.5155*		
142. Chloroprene	$\text{CH}_2=\text{C}(\text{Cl})-\text{CH}=\text{CH}_2$		8.8315 8.7939		
143. Phosgene	COCl_2			11.77179	
144. Di(chloroethyl) ether	$(\text{ClCH}_2\text{CH}_2)_2\text{O}$	9.85 ± 0.03103			
145. Chloroacetone	$\text{CH}_3\text{COCH}_2\text{Cl}$	9.91 ± 0.03102			
146. Dichloroacetone	$\text{CH}_3\text{COCHCl}_2$	10.12 ± 0.03102			
147. Methyl mono-chloroacetate	$\text{ClCH}_2\text{COOCH}_3$	10.35 ± 0.03103			
148. Methyl dichloroacetate	$\text{Cl}_2\text{CHCOOCH}_3$	10.44 ± 0.03103			
149. Ethyl mono-chloroacetate	$\text{ClCH}_2\text{COOC}_2\text{H}_5$	10.20 ± 0.03103			
150. Ethyl trichloroacetate	$\text{Cl}_3\text{CCOOC}_2\text{H}_5$	10.44 ± 0.03103			
151. Methyl bromide	CH_3-Br	10.53 ± 0.0111	11.17154 10.19156 10.80156 10.541133	10.73179 10.633	
152. Ethyl bromide	$\text{CH}_3-\text{CH}_2\text{Br}$	10.24134 10.29 ± 0.0111	10.62154 10.29153	10.49179	10.4766
153. n-Propyl bromide	$\text{C}_3\text{H}_7\text{Br}$	10.18 ± 0.01253		10.29179	10.3566
154. Isopropyl bromide	$(\text{CH}_3)_2\text{CHBr}$	10.075 ± 0.01253		10.11179	10.16; 10.3066
155. n-Butyl bromide	$\text{CH}_3(\text{CH}_2)_3\text{Br}$	10.125 ± 0.111		10.12179	10.2966
156. sec-Butyl bromide	$\text{C}_2\text{H}_5-\text{CH}(\text{Br})-\text{CH}_3$	10.09 ± 0.02253		10.15179	10.18; 10.276
157. Methylene dibromide	CH_2Br_2			10.823	
158. Ethylene dibromide	$\text{BrCH}_2-\text{CH}_2\text{Br}$			10.30179	
159. tert-Butyl bromide	$(\text{CH}_3)_3\text{CBr}$			10.36222	
160. 1,3-Dibromopropane	$\text{Br}-\text{CH}_2-\text{CH}_2-\text{CH}_2\text{Br}$			10.28179	
		*p-electrons of chlorine. **7-electrons.			

Compound	Formula	Ionization potential, eV			
		Photoionization	Spectroscopy	Electron impact	Semi-empirical calculation
161. 1,4-Dibromobutane	$\text{Br}(\text{CH}_2)_4\text{Br}$			10.28179	
162. Vinyl bromide	$\text{H}_2\text{C}=\text{CHBr}$	9.80 ± 0.02116			
163. cis-Dibromoethylene	$\begin{array}{c} \text{H} \quad \text{H} \\ \diagdown \quad / \\ \text{C}=\text{C} \\ / \quad \diagdown \\ \text{Br} \quad \text{Br} \end{array}$	9.45 ± 0.02116			
164. trans-Dibromoethylene	$\begin{array}{c} \text{Br} \quad \text{H} \\ \diagdown \quad / \\ \text{C}=\text{C} \\ / \quad \diagdown \\ \text{H} \quad \text{Br} \end{array}$	9.47 ± 0.02116			
165. Tribromoethylene	$\text{Br}_2\text{C}=\text{CHBr}$	9.27 ± 0.02116			
166. Ethyl monobromoacetate	$\text{BrCH}_2\text{COOC}_2\text{H}_5$	10.13 ± 0.03103			
167. Ethyl monobromobutyrate	$\begin{array}{c} \text{Br}(\text{CH}_2)_3 \\ \diagdown \\ \text{C}=\text{O} \\ / \\ \text{C}_2\text{H}_5-\text{O} \end{array}$	9.85 ± 0.02103			
168. Methyl iodide	CH_3I	9.537 ± 0.0162 9.497134	9.538153	9.67179 9.55233	
169. Ethyl iodide	$\text{CH}_3-\text{CH}_2\text{I}$	9.33 ± 0.0111	9.345153	9.47179	9.5466
170. n-Propyl iodide	$\text{CH}_3-\text{CH}_2-\text{CH}_2\text{I}$	9.26 ± 0.01253		9.41179	9.51; 9.4366
171. n-Butyl iodide	$\text{CH}_3(\text{CH}_2)_3\text{CH}_2\text{I}$	9.21 ± 0.01253		9.32179	9.5; 9.4266
172. n-Pentyl iodide	$\text{CH}_3(\text{CH}_2)_4\text{CH}_2\text{I}$	9.19 ± 0.0111			
173. Methyl mercaptan	CH_3-SH	9.440 ± 0.005253	9.44117		
174. Ethyl mercaptan	$\text{C}_2\text{H}_5-\text{SH}$	9.285 ± 0.005253	9.29117	9.7097	
175. n-Propyl mercaptan	$\text{C}_3\text{H}_7-\text{SH}$	9.195 ± 0.005253	9.16117		
176. tert-Butyl mercaptan	$(\text{CH}_3)_3\text{C}-\text{SH}$		8.79117		
177. Dimethyl sulfide	$(\text{CH}_3)_2\text{S}$	8.685 ± 0.005253	8.73117	9.4097	
178. Diethyl sulfide	$(\text{C}_2\text{H}_5)_2\text{S}$	8.430 ± 0.005253	8.48117	9.3097	
179. Dipropyl sulfide	$(\text{C}_3\text{H}_7)_2\text{S}$	8.30 ± 0.02253		9.2097	
180. Tetramethylene sulfide	$\begin{array}{c} \text{H}_2\text{C}-\text{CH}_2 \\ \quad \diagdown \\ \text{H}_2\text{C}-\text{CH}_2 \quad \text{S} \end{array}$		8.64117		
181. Pentamethylene sulfide	$\begin{array}{c} \text{H}_2\text{C}-\text{CH}_2-\text{CH}_2 \\ \quad \diagdown \quad / \\ \text{H}_2\text{C}-\text{CH}_2-\text{CH}_2 \quad \text{S} \end{array}$		8.46117		
182. Hexamethylene sulfide	$\begin{array}{c} \text{H}_2\text{C}-\text{CH}_2-\text{CH}_2-\text{CH}_2 \\ \quad \diagdown \quad / \quad \diagup \\ \text{H}_2\text{C}-\text{CH}_2-\text{CH}_2 \quad \text{S} \end{array}$		8.36117		

Table XVIII (cont'd)

Compound	Formula	Ionization potential, eV				Compound	Formula	Ionization potential, eV			
		Photoionization	Spectroscopy	Electron impact	Semi-empirical calculation			Photoionization	Spectroscopy	Electron impact	Semi-empirical calculation
183. Thiophene		8.860±0.00525 ^a	8.91117	9.0226		211. Formamide	HCONH ₂	10.16±0.035 ^a	10.2160		
184. 2-Chlorothiophene		8.68±0.0111				212. Acetamide	CH ₃ CONH ₂	9.65±0.035 ^a	19.2117		
185. Hydrogen cyanide	H-CN			13.91179 13.8633		213. N-methylacetamide	CH ₃ CONHCH ₃	8.90±0.0225 ^a	8.82117		
186. Acetonitrile	CH ₃ -CN	12.22±0.0125 ^a	11.96	12.39179		214. N,N-dimethylacetamide	CH ₃ CON(CH ₃) ₂	8.81±0.0525 ^a	8.82117		
187. Propionitrile	CH ₃ -CH ₂ -CN	11.84±0.0225 ^a		11.85179		215. Benzene	C ₆ H ₆	9.245±0.0452 9.24±0.025 ^a	9.24165 9.247181 9.248182 9.240187	9.52179 9.4362 9.21238	
188. Acrylonitrile	CH ₂ =CH-CN	10.91±0.0125 ^a		10.75179		216. Deuterated benzene	C ₆ D ₆		9.254182		
189. Cyanogen	(CN) ₂			13.57181		217. Toluene	C ₆ H ₅ CH ₃	8.82±0.0111 8.81±0.025 ^a	8.822109 8.7797	9.23179 8.7240	
190. Benzonitrile	C ₆ H ₅ -CN			9.95179		218. Ethylbenzene	C ₆ H ₅ C ₂ H ₅	8.76±0.025 ^a	8.7515 8.77108	9.12179	9.1866
191. Cyanogen bromide	Br-CN		10,8156			219. n-Propylbenzene	C ₆ H ₅ -C ₃ H ₇	8.72±0.0211		9.14179	9.1866
192. Cyanogen iodide	I-CN		10,6145			220. Isopropylbenzene	C ₆ H ₅ -CH(CH ₃) ₂	8.69±0.0111	8.615 8.76108	9.13179	9.1866
193. Ammonia	NH ₃	10.15±0.0111 10.25±0.152 10.13±0.02134*	11.58158	10.841 10.52179 11.2170		221. n-Butylbenzene	C ₆ H ₅ -C ₄ H ₉	8.69±0.0111	8.511	9.14179	9.1866
194. Methylamine	CH ₃ -NH ₂	8.97±0.0211		9.897 9.41179		222. Isobutylbenzene	C ₆ H ₅ -CH ₂ CH(CH ₃) ₂	8.69±0.0216		9.19179	
195. Dimethylamine	(CH ₃) ₂ NH	8.24±0.0211	8.4117	9.697 9.5539	8.6766	223. tert-Butylbenzene	C ₆ H ₅ -C(CH ₃) ₃	8.68±0.0216	8.515	9.35179	9.0666
196. Trimethylamine	(CH ₃) ₃ N	7.82±0.0311		9.338	8.0666	224. o-Xylene	C ₆ H ₄ (CH ₃) ₂	8.56±0.0111 8.56±0.025 ^a	8.58108 8.397	8.97187	8.9666
197. Ethylamine	C ₂ H ₅ -NH ₂	8.86±0.0254		9.32179	9.2666	225. m-Xylene	C ₆ H ₄ (CH ₃) ₂	8.56±0.0111 8.59±0.025 ^a	8.315 8.58108	9.02187	
198. n-Propylamine	C ₃ H ₇ -NH ₂	8.78±0.0254		9.17179	9.2466	226. p-Xylene	C ₆ H ₄ (CH ₃) ₂	8.445±0.0152 8.44±0.025 ^a	8.315 8.48108	8.88187	
199. n-Butylamine	C ₄ H ₉ -NH ₂	8.71±0.03254		9.10179	9.2366	227. o-Diethylbenzene	C ₆ H ₄ (C ₂ H ₅) ₂			8.91187	
200. Isopropylamine	(CH ₃) ₂ CH-NH ₂	8.72±0.03254		9.5238		228. m-Diethylbenzene	C ₆ H ₄ (C ₂ H ₅) ₂			8.93187	
201. Isobutylamine	(CH ₃) ₂ CHCH ₂ -NH ₂	8.70±0.025 ^a		9.0179	9.2066	229. p-Diethylbenzene	C ₆ H ₄ (C ₂ H ₅) ₂			8.93157	
202. tert-Butylamine	(CH ₃) ₃ C-NH ₂	8.6425 ^a		9.00218		230. 1,2,3-Trimethylbenzene	C ₆ H ₃ (CH ₃) ₃	8.48±0.0116		8.75187	
203. Diethylamine	(C ₂ H ₅) ₂ NH	8.01±0.01254		9.5238		231. 1,2,4-Trimethylbenzene	C ₆ H ₃ (CH ₃) ₃	8.27±0.02116			
204. Pyrrolidine	(CH ₂) ₄ NH			9.2179		232. 1,3,5-Trimethylbenzene	C ₆ H ₃ (CH ₃) ₃	8.39±0.0211 8.41±0.025 ^a		8.79187	8.7466
205. Isoamylamine	C ₅ H ₁₁ NH ₂			9.5238		233. Durene	C ₆ H ₂ (CH ₃) ₄	8.025±0.0116 8.05±0.025 ^a			8.5366
206. Di-n-propylamine	(n-C ₃ H ₇) ₂ NH	7.84±0.02254		9.5238		234. 1,2,4,5-Tetramethylbenzene	C ₆ H ₂ (CH ₃) ₄	8.03±0.02116			
207. Diisopropylamine	((CH ₃) ₂ CH) ₂ NH	7.73±0.03254		9.4238		235. Pentamethylbenzene	C ₆ H(CH ₃) ₅	7.92±0.025 ^a 7.92±0.02116			8.2666
208. Triethylamine	(C ₂ H ₅) ₃ N	7.50±0.02254		9.1238							
209. Methyl nitrite	CH ₃ ONO			10.7237							
210. Nitromethane	CH ₃ NO ₂	10.08±0.0325 ^a		11.34238							

*Appearance threshold of ions.

Table XVIII (cont'd)

Compound	Formula	Ionization potential, eV			
		Photoionization	Spectroscopy	Electron impact	Semi-empirical calculation
236. Hexamethylbenzene	$C_6(CH_3)_6$	7.85 ± 0.025^8 7.85 ± 0.0211^8			8.1566
237. Styrene	$C_6H_5CH=CH_2$	8.47 ± 0.0225^8	8.35117	8.86179	
238. Phenylacetylene	$C_6H_5C \equiv CH$	8.815 ± 0.00525^8		9.15179	
239. Fluorobenzene	C_6H_5-F	9.19 ± 0.0111	9.19733	9.0211	
240. o-Difluorobenzene	$C_6H_4F_2$	9.31 ± 0.0211^8			
241. p-Difluorobenzene	$C_6H_4F_2$	9.15 ± 0.0211^8			
242. 1,3,5-Tri-fluorobenzene	$C_6H_3F_3$	9.3118			
243. 1,2,4-Tri-fluorobenzene	$C_6H_3F_3$	9.37 ± 0.0211^8			
244. 1,2,3,4-Tetra-fluorobenzene	$C_6H_2F_4$	9.61 ± 0.0211^8			
245. 1,2,3,5-Tetra-fluorobenzene	$C_6H_2F_4$	9.55 ± 0.0211^8			
246. 1,2,4,5-Tetra-fluorobenzene	$C_6H_2F_4$	9.39 ± 0.0211^8			
247. Pentafluorobenzene	C_6HF_5	9.84 ± 0.0211^8			
248. Hexafluorobenzene	C_6F_6	9.97 ± 0.0211^8			
249. p-Fluorotoluene	$C_6H_4CH_3F$	8.78 ± 0.0211^8			
250. α -Fluorotoluene	$C_6H_5CH_2F$	9.12 ± 0.0211^8			
251. α,α -Difluorotoluene	$C_6H_5CHF_2$	9.45 ± 0.0211^8			
252. α,α,α -Trifluorotoluene	$C_6H_5CHF_3$	9.68 ± 0.0211^8	9.683108		
253. 1, α,α,α -Tetrafluorotoluene	$C_6H_4FCF_3$	9.69 ± 0.0211^8			
254. p-Fluoroaniline	$C_6H_4NH_2F$	7.82 ± 0.0211^8			
255. m-Fluoroaniline	$C_6H_4NH_2F$	7.90 ± 0.0211^8			
256. o-Fluoroaniline	$C_6H_4NH_2F$	7.95 ± 0.0211^8			
257. o-Fluorotoluene	$C_6H_4CH_3F$	8.90 ± 0.0211^8			
258. m-Fluorotoluene	$C_6H_4CH_3F$	8.92 ± 0.0211^8			
259. Chlorobenzene	C_6H_5Cl	9.07 ± 0.0211	8.815 (11.297*)	9.42179	
260. o-Dichlorobenzene	$C_6H_4Cl_2$	9.06 ± 0.0211^8		8.3109	
261. p-Dichlorobenzene	$C_6H_4Cl_2$	8.93 ± 0.0211^8			
262. p-Chlorotoluene	$C_6H_4CH_3Cl$	8.69 ± 0.0211			
263. Bromobenzene	C_6H_5Br	8.98 ± 0.0211		9.41179	

Compound	Formula	Ionization potential, eV			
		Photoionization	Spectroscopy	Electron impact	Semi-empirical calculation
264. o-Bromotoluene	$C_6H_4CH_3Br$	8.78 ± 0.0111			
265. p-Bromotoluene	$C_6H_4CH_3Br$	8.67 ± 0.0211			
266. o-Iodobromobenzene	C_6H_4IBr	8.35 ± 0.111			
267. Iodobenzene	C_6H_5I	8.73 ± 0.0311		9.10179	
268. p-Iodotoluene	$C_6H_4CH_3I$	8.50 ± 0.0211^8			
269. Phenol	C_6H_5-OH	8.50 ± 0.0111 8.32 ± 0.0358		9.03179	
270. Benzaldehyde	C_6H_5-CHO	9.51 ± 0.0211 9.60 ± 0.0358		9.82179	
271. Acetophenone	$C_6H_5-COCH_3$	9.65 ± 0.0311^8		9.77179	
272. Benzophenone	$C_6H_5-COC_6H_5$	9.45 ± 0.0311^8			
273. Benzyl methyl ether	$C_6H_5-CH_2-O-CH_3$	8.85 ± 0.0311			
274. Anisole	$C_6H_5-O-CH_3$	9.20 ± 0.0211			
275. Aniline	$C_6H_5-NH_2$	7.70 ± 0.0211 7.69 ± 0.0358			
276. Benzylamine	$C_6H_5-CH_2-NH_2$	8.64 ± 0.0358			
277. Methylaniline	$C_6H_5-NH-CH_3$	7.34 ± 0.0358			
278. Dimethylaniline	$C_6H_5-N(CH_3)_2$	7.14 ± 0.0358			
279. Phenylhydrazine	$C_6H_5-NH-NH_2$	7.62 ± 0.0358			
280. m-Toluidine	$C_6H_4CH_3NH_2$	7.50 ± 0.0358			
281. Quinone	$O=(C_6H_4)=O$	9.67 ± 0.0358			
282. Naphthalene	$C_{10}H_8$	8.12 ± 0.0211 8.14 ± 0.0258		8.111	
283. 1-Methylnaphthalene	$C_{10}H_7-CH_3$	7.96 ± 0.0211		8.015	
284. α -Naphthylamine	$C_{10}H_7-NH_2$	7.30 ± 0.0311^8			
285. β -Naphthylamine	$C_{10}H_7-NH_2$	7.25 ± 0.0311^8			
286. Anthracene	$C_{14}H_{10}$	7.38 ± 0.0311^8			
287. Naphthacene	$C_{18}H_{12}$	6.88 ± 0.0311^8			
288. Pyrrole	$(CH)_4NH$	8.20 ± 0.0125^8		8.90117	8.97215
289. Pyridine	C_5H_5N	9.23 ± 0.0311 9.40 ± 0.0311^8		9.266162	9.839
290. γ -Picoline	$C_5H_4NCH_3$			9.01117	
291. Quinoline	C_8H_7N	8.30 ± 0.0311^8			
292. Acridine	$C_{13}H_9N$	7.78 ± 0.0311^8			
293. Anthraquinone	$C_{14}H_8O_2$	9.34 ± 0.0311^8			
294. Chromium hexacarbonyl	$Cr(CO)_6$	8.03 ± 0.0310^8			
295. Molybdenum hexacarbonyl	$Mo(CO)_6$	8.12 ± 0.0310^8			

*Free electrons of chlorine.

Table XVIII (cont'd)

Compound	Formula	Ionization potential, eV				Compound	Formula	Ionization potential, eV			
		Photoionization	Spectroscopy	Electron impact	Semi-empirical calculation			Photoionization	Spectroscopy	Electron impact	Semi-empirical calculation
296. Tungsten hexacarbonyl	W(CO) ₆	8.18±0.03103				319. Nitrogen dioxide	NO ₂	9.78±0.05253	12.3016 ^a	10.015	
297. Iron pentacarbonyl	Fe(CO) ₅	7.95±0.03103				320. Water	H ₂ O	12.59±0.0111 12.5±0.17 ^a	12.61146 12.5697	12.76179 12.6733	
298. Nickel tetracarbonyl	Ni(CO) ₄	8.28±0.03103				321. Hydrogen peroxide	H ₂ O ₂			12.1220	
299. Rhodamine 6G		7.26±0.05118*				322. Fluorine	F ₂			16.5205	
300. Indigo red		7.32±0.05118*				323. Hydrogen fluoride	HF			16.38205	
301. Indigo blue		7.17±0.05118*				324. Chlorine	Cl ₂	11.48±0.0111		11.80179	
302. Merocyanine		7.2±0.1118*				325. Hydrogen chloride	HCl	12.74±0.0111	12.85154	12.78179	
303. Quinoline blue		7.2±0.1118*				326. Bromine	Br ₂	10.55±0.0211		10.92179	
304. Pinacyanole		7.1±0.1118*				327. Hydrogen bromide	HBr	11.62±0.0111	11.9311	11.63179	
305. Di (cyclopentadienyl) chromium	Cr(C ₅ H ₅) ₂			6.91248		328. Iodine	I ₂	9.28±0.0211		9.41179	
306. Di (cyclopentadienyl) vanadium	V(C ₅ H ₅) ₂			7.56246		329. Hydrogen iodide	HI	10.38±0.0211	10.39154	10.48179	
307. Di (cyclopentadienyl) magnesium	Mg(C ₅ H ₅) ₂			7.76246		330. Sulfur	S ₂			10.8199	
308. Di (cyclopentadienyl) nickel	Ni(C ₅ H ₅) ₂			7.06246		331. Hydrogen sulfide	H ₂ S	10.458±0.0152	10.473146 10.4297	10.4170 10.533	
309. Di (cyclopentadienyl) cobalt	Co(C ₅ H ₅) ₂			6.2218		332. Carbon disulfide	CS ₂	10.080±0.0152 10.129±0.0152*	10.079157 10.137157*	10.13234	
310. Di (cyclopentadienyl) iron	Fe(C ₅ H ₅) ₂			7.05246		333. Sulfur monoxide	SO			10.7171	
311. Di (cyclopentadienyl) manganese	Mn(C ₅ H ₅) ₂			7.25218		334. Sulfur dioxide	SO ₂	12.42±0.02134 12.34±0.0211	12.05157	13.1147	
Inorganic compounds						335. Hydrogen selenide	H ₂ Se		9.741	10.1219	
312. Hydrogen	H ₂	15.4278	15.427139 ^a	15.44169 15.9170		336. Hydrogen telluride	H ₂ Te		9.141		
313. Oxygen	O ₂	12.1±0.178 12.075±0.0111	12.211	13.0170 12.1244		337. Lithium iodide	LiI			8.55163	
314. Nitrogen	N ₂	15.5190 15.5812	15.581167 15.57628	16.5170 15.9033		338. Sodium	Na		5.138119	5.15217	
315. Carbon monoxide	CO	14.01±0.0111	13.9227 14.013251	14.1170		339. Sodium iodide	NaI			8.8223	
316. Carbon dioxide	CO ₂	13.79±0.0111 14.0±0.378	13.73166 13.79157	14.4170 13.85198		340. Sodium azide	NaN ₃			11.7231	
317. Nitric oxide	NO	9.20±0.0391 9.25±0.0252	9.24136	9.3170 9.4244		341. Potassium	K		4.339119	4.34217	
318. Nitrous oxide	N ₂ O	12.90±0.0111 12.83±0.0791	12.72252 12.9428	12.9170 12.9245		342. Potassium iodide	KI			8.3223	
						343. Rubidium	Rb		4.176119	4.18217	
						344. Cesium	Cs		3.893119	3.19217	
						345. Mercury	Hg		10.434119	10.43235	
						346. Boron trichloride	BCl ₃			12.0242	
						347. Aluminum	Al		5.98119	6.1218	

*Appearance threshold of ions

*Second ionization potential.

Table XVIII (cont'd)

Compound	Formula	Ionization potential, eV			
		Photo-ionization	Spectroscopy	Electron impact	Semi-empirical calculation
348. Aluminum hemioxide	Al ₂ O			7.7218	
349. Europium	Eu			6.08246*	
350. Terbium	Tb			5.98248*	
351. Cerium	Ce			5.60248*	
352. Thorium	Th			6.95248*	
353. Monosilane	SiH ₄			12.2249	
354. Silicon monoxide	SiO			10.840	
355. Silicon dioxide	SiO ₂			11.740	
356. Silicon tetrachloride	SiCl ₄			11.6186	
357. Titanium trichloride	TiCl ₃			13.0159	
358. Titanium tetrachloride	TiCl ₄			11.7159	
359. Monogermane	GeH ₄			12.3249	
360. Phosphine	PH ₃			10.0249	
361. Phosphorus trichloride	PCl ₃			12.3200	
362. Arsenic trichloride	AsCl ₃			12.4200	
363. Antimony trichloride	SbCl ₃			11.5200	
364. Uranium tetrachloride	UCl ₄			11.5217	
Radicals					
365. Hydrogen (atomic)	H		13.595141	13.62202	
366. Carbon (atomic)	C		11.264119	11.1191	
367. Methine	CH			11.1333	
368. Methylene	CH ₂		10.396143	11.9195, 196	
369. Methyl	CH ₃		9.840142	9.68213 10.07203 10.11204 9.85196 9.95192, 188	
370. Ethyl	CH ₃ -CH ₂			8.67203 8.78192	
371. n-Propyl	CH ₃ -CH ₂ -CH ₂			8.69±0.05208 7.94±0.05207 7.80203	8.5843 8.68208 8.5199
372. Isopropyl	CH ₃ -CH-CH ₃			7.90±0.05208 7.77203 7.45178	7.8143 7.98208 7.7699
*Surface-ionization method.					
Compound	Formula	Ionization potential, eV			
		Photo-ionization	Spectroscopy	Electron impact	Semi-empirical calculation
373. n-Butyl	CH ₃ -(CH ₂) ₂ -CH ₂			8.64±0.05208	8.5713 8.64208 8.4799
374. Isobutyl	(CH ₃) ₂ -CH-CH ₂			8.35±0.05208	8.4213 8.55208
375. sec-Butyl	CH ₃ -CH ₂ -CH-CH ₃			7.93±0.05208	7.7613 7.87208 7.6799
376. tert-Butyl	(CH ₃) ₃ C			7.42±0.05208 7.19203 6.9178	7.1913 7.32208 6.9409
377. n-Pentyl	CH ₃ -(CH ₂) ₃ -CH ₂				8.4999
378. sec-Amyl	CH ₃ -(CH ₂) ₂ -CH-CH ₃				7.6699
379. tert-Amyl	CH ₃ -CH ₂ -C-(CH ₃) ₂				6.9499
380. sec-Heptyl	C ₃ H ₇ -CH-C ₃ H ₇				7.5699
381. Allyl	CH ₂ =CH-CH ₂			8.16±0.03183 8.25±0.08192	
382. Fluoromethyl	CH ₂ F			9.35208	
383. Difluoromethyl	CHF ₂			9.45208	
384. Trifluoromethyl	CF ₃			10.2: 10.1208 8.9182	
385. Fluorine (atomic)	F		17.422119		
386. Chlorine (atomic)	Cl		12.959119		
387. Chloromethyl	CH ₂ Cl			9.32±0.05208 9.70±0.09212	
388. Dichloromethyl	CHCl ₂			9.30208 9.54212	
389. Trichloromethyl	CCl ₃			8.78208	
390. Bromine (atomic)	Br		11.844119		
391. Bromoethyl	CH ₂ Br			9.30208 8.34212	
392. Dibromomethyl	CHBr ₂			8.13±0.16212	
393. Iodine (atomic)	I		10.44119		
394. Sulfur (atomic)	S		10.357119		
395. Sulfhydryl	HS			11.1198	
396. Thiocarbonyl	CS			10.7199	
397. Oxygen (atomic)	O		13.615119		
398. Hydroxyl	OH			13.733	
399. Nitrogen (atomic)	N		14.545119		
400. Monocyanogen	CN			14.0181	
401. Peroxyhydroxyl	HO ₂			11.53197	
402. Imine	NH			13.1211	
403. Amine	NH ₂			11.4210	

Table XVIII (cont'd)

Compound	Formula	Ionization potential, eV			
		Photo-ionization	Spectroscopy	Electron impact	Semi-empirical calculation
404.	N ₂ H ₂			9.85 ± 0.1 ²¹⁰	
405. Hydrazyl	N ₂ H ₃			7.88 ± 0.2 ²¹⁰	
406.	CH ₃ -N-NH ₂			5.07 ²¹³	
407.	CH ₃ -NH-NH			5.12 ²¹³	
408.	CH ₃ -N-NH			5.29 ²¹³	
409.	(CH ₃) ₃ N ₂			4.95 ²¹³	
410. Phenyl	C ₆ H ₅			9.89 ¹⁸⁷	
411. Benzyl	C ₆ H ₅ -CH ₂			7.73 ¹⁸⁸ 7.81 ¹⁸⁹	
412.	p-C ₆ H ₄ CH ₂ CH ₂			7.46 ¹⁹⁰	
413.	o-C ₆ H ₄ CH ₂ CH ₂			7.61 ¹⁹⁰	
414.	m-C ₆ H ₄ CH ₂ CH ₂			7.65 ¹⁹⁰	
415. Diphenylmethyl	C ₆ H ₅ -CH-C ₆ H ₅			7.32 ²³²	
416. β-Naphthylmethyl	C ₁₀ H ₇ CH ₂			7.56 ²³²	
417. α-Naphthylmethyl	C ₁₀ H ₇ CH ₂			7.35 ²³²	

resonance absorption lines of Kr due to the high pressure, which increases the yield of ions. At high NO pressures, there are enough NO molecules to deactivate almost all the excited krypton atoms, and addition of H₂, D₂, or He only results in broadening of the krypton absorption lines, with a resultant increase in the number of excited krypton atoms, leading to an increase in the ion current.

12. SUMMARY OF THE FIRST ADIABATIC IONIZATION POTENTIALS OF MOLECULAR GASES AND VAPORS

Table XVIII, which is given below, includes all the values existing in the literature of the first adiabatic ionization potentials of molecules that have been measured by the photoionization or the spectroscopic method. Since many important compounds have not yet been studied by these methods, columns 6 and 7 give the first ionization potentials determined by the electron-impact method or by semi-empirical calculations. These data often differ quite significantly from the adiabatic ionization potentials, but can be useful for various estimates. The table also includes the first ionization potentials of free radicals. Almost all the molecular radicals have been studied by the electron-impact method using mass-spectrometric technique. The values of the ionization potentials given for them may differ from the adiabatic values. The values of the ionization potentials of atomic radicals are known with high accuracy, since most of them have been determined by the spectroscopic method.*

*See also the handbook, *Énergii razryva khimicheskikh svyazei. Potentsialy ionizatsii i srodstvo k élektronu* (Dissociation Energies of Chemical Bonds. Ionization Potentials and Electron Affinities), Ed. V. K. Kondrat'ev, AN SSSR (1963).

Note added in proof. Watanabe and his associates^[255] give a list of I_p values obtained by the photoionization method. It was published after I wrote this article, and unfortunately I could include only part of these data in Table XVIII. A number of excellent studies have been published during the last year and a half on photoionization of gases and vapors, and I have not discussed them in this article for the same reason.

¹On the Threshold of Space. Proceedings of the Conference on Chemical Aeronomy, Cambridge (U.S.A., 1956); (Russ. Transl.), IL (1960); M. Nicolet, *Handbuch der Physik*, Vol. 49, Springer-Verlag, Berlin (1958).

²E. Burgess, *Frontier to Space*, Chapman and Hall, London, 1955; Ya. L. Al'pert, *UFN* 71, 369 (1960); *Soviet Phys. Uspekhi* 3, 479 (1961).

³N. A. Kaptsov, *Élektricheskie yavleniya v gazakh i v vakuume* (Electrical Phenomena in Gases and in Vacuo), Gostekhizdat (1950); German Transl., Deutscher Verlag der Wissenschaften, Berlin (1955); L. B. Loeb, *Fundamental Processes of Electrical Discharge in Gases*, Wiley, New York (1939); Russ. Transl., Gostekhizdat (1950); V. L. Granovskii, *Élektricheskiĭ tok v gazakh* (The Electrical Current in Gases), Vol. I, (1952).

⁴A. R. Knudson and J. E. Kupperian, Jr, *J. Opt. Soc. Amer.* 47, 440 (1957); T. A. Chubb and H. Fridman, *Rev. Sci. Instr.* 26, 494 (1955).

⁵A. D. Walsh, *Contribution to the Study of Molecular Structure. Dedicated to the Memory of Victor Henri*. Ed. M. de Hemtinne, Desoer, Liège (1947-1948), p. 191.

⁶F. P. Lossing and I. Tanaka, *J. Chem. Phys.* 25, 1031 (1956).

⁷Vilesov, Kurbatov, and Terenin, *DAN SSSR* 122, 94 (1958).

⁸F. I. Vilesov and M. E. Akopyan, *PTÉ* No. 5, 145 (1962).

⁹A. N. Terenin, *UFN* 11, 276 (1931).

- ¹⁰E. C. Y. Inn, *Spectrochim. Acta* **7**, 65 (1955).
¹¹K. Watanabe, *J. Chem. Phys.* **26**, 542 (1957).
¹²G. L. Weissler, *Handbuch der Physik*, Vol. 21, p. 304, Springer-Verlag (1956).
¹³J. C. Boyce, *Revs. Modern Phys.* **13**, 1 (1941).
¹⁴H. Spöner and E. Teller, *Revs. Modern Phys.* **13**, 75 (1941).
¹⁵W. C. Price, *Chem. Revs.* **41**, 257 (1947).
¹⁶Price, Bralsford, Harris, and Ridley, *Spectrochim. Acta* **14**, 45 (1959).
¹⁷W. C. Price, *Advances in Spectroscopy* **1**, 56 (1959).
¹⁸P. G. Wilkinson, *J. Mol. Spectr.* **6**, 1 (1961).
¹⁹P. Lenard, *Ann. Phys.* **1**, 486 (1900); **3**, 298 (1900); **8**, 149 (1902).
²⁰F. Bloch, *Compt. rend.* **146**, 892 (1908).
²¹A. L. Hughes, *Proc. Cambridge Phil. Soc.* **15**, 483 (1910).
²²F. Palmer, *Phys. Rev., Ser. 1*, **32**, 1 (1911).
²³P. Lenard and C. Ramsauer, *Sitzungsber. Heidelberg. Akad. Wiss.* **1A**, Nos. 28, 31, 32; **2A**, Nos. 16, 24 (1911).
²⁴A. Martin, *ibid.* **9A**, No. 10 (1918).
²⁵A. L. Hughes and L. A. DuBridge, *Photoelectric Phenomena*, McGraw-Hill, New York (1932).
²⁶R. E. Worley, *Phys. Rev.* **64**, 207 (1943).
²⁷G. Herzberg, *Molecular Spectra and Molecular Structure. I. Diatomic Molecules*, Prentice-Hall, New York (1939).
²⁸F. G. Houtermans, *Z. Phys.* **41**, 619 (1927).
²⁹J. Stark, *Phys. Z.* **10**, 614 (1909).
³⁰S. V. Serkov, *ZhRfKhO* **44**, 293 (1912).
³¹C. B. Gudden, *Lichtelectrische Erscheinungen (Photoelectric Phenomena)* (1928), p. 231.
³²E. C. Allberry, *Phil. Mag.* **14**, 400 (1932).
³³F. H. Field and J. L. Franklin, *Electron Impact Phenomena and the Properties of Gaseous Ions*, Academic Press, New York (1957).
³⁴G. P. Barnard, *Modern Mass Spectrometry*, Inst. of Physics, London (1953); *Russ. Transl.*, IL, 1957.
³⁵K. T. Compton and C. C. Van Voorhis, *Phys. Rev.* **27**, 724 (1926).
³⁶W. C. Price and W. T. Tutte, *Proc. Roy. Soc.* **A174** 207 (1940).
³⁷W. C. Price and A. D. Walsh, *Proc. Roy. Soc.* **A174**, 220 (1940); **A179**, 201 (1941).
³⁸A. D. Walsh, *Proc. Roy. Soc.* **A185**, 176 (1946).
³⁹W. C. Price and A. D. Walsh, *Proc. Roy. Soc.* **A185**, 182 (1946).
⁴⁰Porter, Chupka, and Inghram, *J. Chem. Phys.* **23**, 216 (1955).
⁴¹W. C. Price, *J. Chem. Phys.* **16**, 551 (1948).
⁴²Hurzeler, Inghram, and Morrison, *ibid.* **28**, 76 (1958).
⁴³D. P. Stevenson, *The Energies of Hydrocarbon Radicals and Their Ions*, No. 29, p. 19, Symposium at Am. Chem. Soc. Meeting, Kansas City (March, 1954).
⁴⁴Hurzeler, Inghram, and Morrison, *J. Chem. Phys.* **27**, 313 (1957).
⁴⁵R. J. Kandel, *Phys. Rev.* **91**, 436 (1953).
⁴⁶Weissler, Samson, Ogawa, and Cook, *J. Opt. Soc. Amer.* **49**, 338 (1959).
⁴⁷Vilesov, Kurbatov, and Terenin, *DAN SSSR* **138**, 1329 (1961); *Soviet Phys. Doklady* **6**, 490 (1961).
⁴⁸Kurbatov, Vilesov, and Terenin, *ibid.* **140**, 797 (1961); *Soviet Phys. Doklady* **6**, 883 (1962).
⁴⁹E. P. Wigner, *Phys. Rev.* **73**, 1002 (1948).
⁵⁰S. Geltman, *ibid.* **102**, 171 (1956).
⁵¹G. H. Wannier, *ibid.* **100**, 1180 (1955).
⁵²K. Watanabe, *J. Chem. Phys.* **22**, 1564 (1954).
⁵³H. J. Braddick and R. W. Ditchburn, *Proc. Roy. Soc.* **A143**, 472 (1934).
⁵⁴Ditchburn, Jutsum, and Marr, *ibid.* **A219**, 89 (1953).
⁵⁵Po Lee and G. L. Weissler, *Phys. Rev.* **99**, 540 (1955).
⁵⁶Po Lee and G. L. Weissler, *Proc. Roy. Soc.* **A219**, 71 (1953).
⁵⁷Morrison, Hurzeler, Inghram, and Stanton, *J. Chem. Phys.* **33**, 821 (1960).
⁵⁸F. I. Vilesov and A. N. Terenin, *DAN SSSR* **115**, 744 (1957).
⁵⁹Akopyan, Vilesov, and Terenin, *ibid.* **140**, 1037 (1961); *Soviet Phys. Doklady* **6**, 890 (1962).
⁶⁰G. G. Hall, *Proc. Roy. Soc.* **A205**, 541 (1951).
⁶¹J. Lennard-Jones and G. G. Hall, *Disc. Faraday Soc.* **10**, 18 (1951).
⁶²R. E. Honing, *J. Chem. Phys.* **16**, 105 (1948).
⁶³G. G. Hall, *Proc. Roy. Soc.* **A213**, 102 (1952).
⁶⁴G. G. Hall, *Trans. Faraday Soc.* **49**, 113 (1953).
⁶⁵G. G. Hall, *ibid.* **50**, 319 (1954).
⁶⁶J. L. Franklin, *J. Chem. Phys.* **22**, 1304 (1954).
⁶⁷J. Tunstead, *Proc. Phys. Soc. London* **A66**, 304 (1953).
⁶⁸Ditchburn, Tunstead, and Yates, *Proc. Roy. Soc.* **A181**, 386 (1943).
⁶⁹P. J. Jutsum, *Proc. Phys. Soc. London* **A67**, 190 (1954).
⁷⁰R. W. Ditchburn and G. V. Marr, *ibid.* **A66**, 655 (1953).
⁷¹F. L. Mohler and C. Boeckner, *J. Res. Nat. Bur. Standards* **3**, 303 (1929).
⁷²H. Beutler, *Z. Phys.* **93**, 177 (1935).
⁷³C. E. Moore, *Atomic Energy Levels*, Vol. 1, Circular No. 467, Nat. Bur. of Standards, Washington, D. C. (1949).
⁷⁴G. V. Marr, *Proc. Roy. Soc.* **A224**, 83 (1954).
⁷⁵G. V. Marr, *Proc. Phys. Soc. London* **A67**, 196 (1954).
⁷⁶Dorman, Morrison, and Nicholson, *J. Chem. Phys.* **32**, 378 (1960).
⁷⁷A. Dalgarno, *Proc. Phys. Soc. London* **A65**, 663 (1952).
⁷⁸Wainfan, Walker, and Weissler, *Phys. Rev.* **99**, 542 (1955).

- ⁷⁹ M. J. Seaton, Proc. Roy. Soc. A208, 408 (1951); Proc. Phys. Soc. London A67, 927 (1954).
- ⁸⁰ J. A. Wheeler, Phys. Rev. 43, 258 (1933).
- ⁸¹ J. P. Vinti, *ibid.* 44, 524 (1933).
- ⁸² B. Trumphy, Z. Physik 71, 720 (1931).
- ⁸³ J. Hargreaves, Proc. Cambridge Phil. Soc. 25, 75 (1928).
- ⁸⁴ A. L. Stewart, Proc. Phys. Soc. London A67, 917 (1954).
- ⁸⁵ M. J. Seaton, Proc. Roy. Soc. A208, 418 (1951).
- ⁸⁶ D. R. Bates, Monthly Notices Roy. Astron. Soc. 106, 423 (1946).
- ⁸⁷ D. R. Bates and H. S. W. Massey, Proc. Roy. Soc. A177, 329 (1941).
- ⁸⁸ A. W. Ehler and G. L. Weissler, J. Opt. Soc. Amer. 45, 1035 (1955).
- ⁸⁹ D. R. Bates and M. J. Seaton, Monthly Notices Roy. Astron. Soc. 109, 698 (1949).
- ⁹⁰ Wainfan, Walker, and Weissler, J. Appl. Phys. 24, 1318 (1953).
- ⁹¹ W. C. Walker and G. L. Weissler, J. Chem. Phys. 23, 1962 (1955).
- ⁹² W. C. Walker and G. L. Weissler, *ibid.* 23, 1540 (1955).
- ⁹³ W. C. Walker and G. L. Weissler, *ibid.* 23, 1547 (1955).
- ⁹⁴ Steiner, Giese, and Inghram, *ibid.* 34, 189 (1961).
- ⁹⁵ W. C. Price, Phys. Rev. 47, 444 (1935).
- ⁹⁶ J. P. Teegan and A. D. Walsh, Trans. Faraday Soc. 47, 1 (1951).
- ⁹⁷ Sugden, Walsh, and Price, Nature 148, 373 (1941).
- ⁹⁸ F. D. Rossini, J. Res. Natl. Bur. Standards 12, 735 (1934).
- ⁹⁹ V. M. Baranov and T. K. Rebane, Optika i Spektroskopiya 8, 268 (1960); Engl. Transl. (Opt. Soc. Amer.), p. 138.
- ¹⁰⁰ O. A. Reutov, Teoreticheskie problemy organicheskoi khimii (Theoretical Problems of Organic Chemistry), MGU (1956).
- ¹⁰¹ W. C. Price, J. Chem. Phys. 3, 256 (1935).
- ¹⁰² F. I. Vilesov, DAN SSSR 132, 1332 (1960).
- ¹⁰³ F. I. Vilesov and B. L. Kurbatov, *ibid.* 140, 1364 (1961).
- ¹⁰⁴ W. C. Price, Annual Repts. Prog. Chem., Chem. Soc. 36, 47 (1939).
- ¹⁰⁵ W. C. Price and R. W. Wood, J. Chem. Phys. 3, 439 (1935).
- ¹⁰⁶ A. D. Walsh, Annual Repts. Prog. Chem., Chem. Soc. 44, 32 (1947).
- ¹⁰⁷ W. C. Price and R. W. Wood, J. Chem. Phys. 3, 339 (1935).
- ¹⁰⁸ Hammond, Price, Teegan, and Walsh, Disc. Faraday Soc. 9, 53 (1950).
- ¹⁰⁹ W. C. Price and A. D. Walsh, Proc. Roy. Soc. A191, 22 (1947).
- ¹¹⁰ F. I. Vilesov, Zhur. Fiz. Khim. 35, 2010 (1961).
- ¹¹¹ G. N. Lewis and D. Lipkin, J. Am. Chem. Soc. 64, 2801 (1942).
- ¹¹² A. I. Sidorova and A. N. Terenin, Izv. AN SSSR, Otd. Khim. Nauk, No. 2, 152 (1950).
- ¹¹³ A. I. Sidorova, DAN SSSR 72, 327 (1950).
- ¹¹⁴ A. I. Sidorova, Zhur. Fiz. Khim. 28, 525 (1954).
- ¹¹⁵ Scheibe, Brück, and Dörr, Chem. Ber. 85, 867 (1952).
- ¹¹⁶ Bralsford, Harris, and Price, Proc. Roy. Soc. A258, 459 (1960).
- ¹¹⁷ L. Issaacs, W. C. Price, and R. Ridley, see Ref. 1, p. 204.
- ¹¹⁸ F. I. Vilesov, DAN SSSR 132, 632 (1960).
- ¹¹⁹ Zaïdel', Prokof'ev, and Raïskii, Tablitsa spektral'nykh liniï (Tables of Spectrum Lines), M. Gostekhizdat (1952); Engl. Transl., Pergamon Press, New York (1961).
- ¹²⁰ A. N. Terenin and B. Popov, Phys. Z. Sowjetunion 2, 299 (1932).
- ¹²¹ R. F. Herzog and F. F. Marmo, J. Chem. Phys. 27, 1202 (1957).
- ¹²² E. Schönheit, Z. Phys. 149, 153 (1957).
- ¹²³ W. A. Chupka, J. Chem. Phys. 30, 191 (1959).
- ¹²⁴ Higasi, Omura, and Baba, Nature 178, 652 (1956).
- ¹²⁵ M. E. Akopyan and F. I. Vilesov, Kinetika i Kataliz 4, 39 (1963).
- ¹²⁶ I. Tanaka and E. W. R. Steacie, J. Chem. Phys. 26, 715 (1957).
- ¹²⁷ V. L. Lëvshin, Fotoluminestsentsiya zhidkikh i tverdykh veshchestv (Photoluminescence of Liquid and Solid Substances), Gostekhizdat (1951).
- ¹²⁸ P. Pringsheim, Fluorescence and Phosphorescence, Interscience, New York (1949); Russ. Transl., IL, (1951).
- ¹²⁹ I. Tanaka and E. W. R. Steacie, Can. J. Chem. 35, 821 (1957).
- ¹³⁰ E. W. R. Steacie and D. J. Leroy, J. Chem. Phys. 11, 164 (1943).
- ¹³¹ Smith, Stewart, and Taylor, Can. J. Chem. 32, 961 (1954).
- ¹³² F. I. Vilesov and A. N. Terenin, DAN SSSR 133, 1060 (1960).
- ¹³³ F. I. Vilesov and A. N. Terenin, *ibid.* 134, 71 (1960).
- ¹³⁴ E. C. Y. Inn, Phys. Rev. 91, 1194 (1953).
- ¹³⁵ K. Watanabe and T. Namioka, J. Chem. Phys. 24, 915 (1956).
- ¹³⁶ Watanabe, Marmo, and Inn, Phys. Rev. 91, 1155 (1953).
- ¹³⁷ A. E. Gillam and E. S. Stern, An Introduction to Electronic Absorption Spectroscopy in Organic Chemistry, Arnold, London (1954); Russ. Transl., IL (1957).
- ¹³⁸ E. J. Bowen, Quart. Rev. 4, 236 (1950).
- ¹³⁹ H. Beutler and H. O. Junger, Z. Physik 100, 80 (1936).
- ¹⁴⁰ see Refs. 36, 37.
- ¹⁴¹ R. T. Birge, Phys. Rev. 52, 241 (1937).
- ¹⁴² G. Herzberg and J. Shoosmith, Can. J. Phys. 34, 523 (1956).
- ¹⁴³ G. Herzberg, *ibid.* 39, 1511 (1961).

- ¹⁴⁴ T. M. Sugden and A. D. Walsh, *Trans. Faraday Soc.* **41**, 76 (1945).
- ¹⁴⁵ W. C. Price and A. D. Walsh, *ibid.* **41**, 381 (1945).
- ¹⁴⁶ W. C. Price, *J. Chem. Phys.* **4**, 147 (1936).
- ¹⁴⁷ H. D. Smyth and D. M. Mueller, *Phys. Rev.* **43**, 121 (1933).
- ¹⁴⁸ A. D. Walsh, *Trans. Faraday Soc.* **43**, 158 (1947).
- ¹⁴⁹ W. A. Noyes, Jr., *J. Chem. Phys.* **3**, 430 (1935).
- ¹⁵⁰ A. B. F. Duncan, *ibid.* **3**, 131 (1935); **8**, 444 (1940).
- ¹⁵¹ A. D. Walsh, *Trans. Faraday Soc.* **41**, 498 (1945).
- ¹⁵² A. D. Walsh, *ibid.* **42**, 56 (1946).
- ¹⁵³ W. C. Price, *J. Chem. Phys.* **4**, 539 (1936).
- ¹⁵⁴ W. C. Price, *Proc. Roy. Soc.* **A167**, 216 (1938).
- ¹⁵⁵ A. D. Walsh, *Trans. Faraday Soc.* **41**, 35 (1945).
- ¹⁵⁶ A. D. Walsh, *ibid.* **43**, 60 (1947).
- ¹⁵⁷ W. C. Price and D. M. Simpson, *Proc. Roy. Soc.* **A165**, 272 (1938).
- ¹⁵⁸ Y. Tanaka et al., *Science of Light (Japan)* **8**, 80 (1951).
- ¹⁵⁹ Marriot, Thorburn, and Craggs, *Proc. Roy. Soc.* **B67**, 437 (1954).
- ¹⁶⁰ H. D. Hunt, *J. Am. Chem. Soc.* **75**, 18 (1953).
- ¹⁶¹ P. G. Wilkinson, *Can. J. Phys.* **34**, 596 (1956).
- ¹⁶² El-Sayed, Kaska, and Tanaka, *J. Chem. Phys.* **34**, 334 (1961).
- ¹⁶³ L. Friedman, *ibid.* **23**, 477 (1955).
- ¹⁶⁴ L. E. Lyons and G. C. Morris, *J. Mol. Spectr.* **4**, 480 (1960).
- ¹⁶⁵ Y. Tanaka and T. Takamine, *Sci. Papers Inst. Phys. Chem. Res. Tokyo* **39**, 427 (1942).
- ¹⁶⁶ G. B. Sabine, *Phys. Rev.* **55**, 1064 (1939).
- ¹⁶⁷ R. E. Worley and F. A. Jenkins, *Phys. Rev.* **54**, 305 (1938).
- ¹⁶⁸ W. C. Price and D. M. Simpson, *Trans. Faraday Soc.* **37**, 106 (1941).
- ¹⁶⁹ L. G. Smith and W. Bleakney, *Phys. Rev.* **49**, 883 (1936).
- ¹⁷⁰ H. D. Smyth, *Revs. Modern Phys.* **3**, 347 (1931).
- ¹⁷¹ L. G. Smith, *Phys. Rev.* **51**, 263 (1937).
- ¹⁷² M. B. Koffel and R. A. Lad, *J. Chem. Phys.* **16**, 420 (1948).
- ¹⁷³ J. A. Hipple, Jr., *Phys. Rev.* **53**, 530 (1938).
- ¹⁷⁴ D. P. Stevenson and J. A. Hipple, Jr., *J. Am. Chem. Soc.* **64**, 1588 (1942).
- ¹⁷⁵ J. Delfosse and W. Bleakney, *Phys. Rev.* **56**, 256 (1939).
- ¹⁷⁶ F. H. Field, *J. Chem. Phys.* **20**, 1734 (1952).
- ¹⁷⁷ see Ref. 174.
- ¹⁷⁸ D. P. Stevenson, *Disc. Faraday Soc.* **10**, 35 (1951).
- ¹⁷⁹ J. D. Morrison and A. J. C. Nicholson, *J. Chem. Phys.* **20**, 1021 (1952).
- ¹⁸⁰ J. Hissel, *Bull. Soc. Roy. sci. Liège* **21**, 457 (1952).
- ¹⁸¹ C. A. McDowell and J. W. Warren, *Trans. Faraday Soc.* **48**, 1084 (1952).
- ¹⁸² Dibeler, Reese, and Mohler, *J. Chem. Phys.* **20**, 761 (1952).
- ¹⁸³ H. Branson and C. Smith, *J. Am. Chem. Soc.* **75**, 4133 (1953).
- ¹⁸⁴ J. P. Blewett, *Phys. Rev.* **49**, 900 (1936).
- ¹⁸⁵ D. P. Stevenson, *J. Chem. Phys.* **18**, 1347 (1950).
- ¹⁸⁶ R. H. Vought, *Phys. Rev.* **71**, 93 (1947).
- ¹⁸⁷ F. H. Field and J. L. Franklin, *J. Chem. Phys.* **22**, 1895 (1954).
- ¹⁸⁸ Lossing, Ingold, and Henderson, *J. Chem. Phys.* **22**, 621 (1954).
- ¹⁸⁹ Farmer, Henderson, McDowell, and Lossing, *ibid.* **22**, 1948 (1954).
- ¹⁹⁰ Farmer, Lossing, Marsden, and McDowell, *ibid.* **24**, 52 (1956).
- ¹⁹¹ W. A. Chupka and M. G. Inghram, *J. Chem. Phys.* **21**, 371 (1953).
- ¹⁹² J. B. Farmer and F. P. Lossing, *Can. J. Chem.* **33**, 861 (1955).
- ¹⁹³ Lossing, Ingold, and Henderson, *The Study of Free Radicals by Mass Spectrometry*, Institute of Petroleum, London (1953), p. 102.
- ¹⁹⁴ F. A. Long and L. Friedman, *J. Am. Chem. Soc.* **75**, 2837 (1953).
- ¹⁹⁵ A. Langer and J. A. Hipple, *Phys. Rev.* **69**, 691 (1946).
- ¹⁹⁶ Langer, Hipple, and Stevenson, *J. Chem. Phys.* **22**, 1836 (1954).
- ¹⁹⁷ S. N. Foner and R. L. Hudson, *J. Chem. Phys.* **23**, 1364 (1955).
- ¹⁹⁸ J. L. Franklin and H. E. Lumpkin, *J. Am. Chem. Soc.* **74**, 1023 (1952).
- ¹⁹⁹ H. D. Smyth and J. P. Blewett, *Phys. Rev.* **46**, 276 (1934).
- ²⁰⁰ Kusch, Hustrulid, and Tate, *ibid.* **52**, 843 (1937).
- ²⁰¹ Mann, Hustrulid, and Tate, *ibid.* **58**, 340 (1940).
- ²⁰² W. Bleakney, *ibid.* **35**, 1180 (1930).
- ²⁰³ J. A. Hipple and D. P. Stevenson, *Phys. Rev.* **63**, 121 (1943); A. G. Evans, *Trans. Faraday Soc.* **42**, 719 (1946).
- ²⁰⁴ J. D. Waldron, *Trans. Faraday Soc.* **50**, 102 (1954).
- ²⁰⁵ J. F. Borns, *The Heat of Dissociation of N₂ and the Appearance Potential of Some Ions Formed in F₂ and HF by Electron Impact*, Carbon Chemicals Co., Report K-1147, Oct. 8, 1954.
- ²⁰⁶ J. W. Warren and J. D. Craggs, *Mass Spectrometry*, London (1952), p. 36.
- ²⁰⁷ D. P. Stevenson, *Trans. Faraday Soc.* **49**, 867 (1953).
- ²⁰⁸ F. P. Lossing, *Advances in Mass Spectrometry*, Vol. 1, Pergamon, New York (1959), p. 431.
- ²⁰⁹ R. F. Baker and J. T. Tate, *Phys. Rev.* **55**, 236 (1939).
- ²¹⁰ S. N. Foner and R. L. Hudson, *J. Chem. Phys.* **29**, 442 (1958).
- ²¹¹ R. I. Reed and W. Snedden, *J. Chem. Soc.*, 4132 (1959).
- ²¹² R. I. Reed and W. Snedden, *Trans. Faraday Soc.* **55**, 876 (1959).
- ²¹³ see Ref. 208, p. 443.
- ²¹⁴ D. P. Stevenson, *J. Am. Chem. Soc.* **65**, 209 (1943).

- ²¹⁵ Omura, Baba, and Higasi, *J. Phys. Soc. Japan* **10**, 317 (1955).
- ²¹⁶ J. Delfosse and W. Bleakney, *Phys. Rev.* **56**, 256 (1939).
- ²¹⁷ J. T. Tate and P. T. Smith, *Phys. Rev.* **46**, 773 (1934).
- ²¹⁸ Porter, Schissel, and Inghram, *J. Chem. Phys.* **23**, 339 (1955).
- ²¹⁹ J. L. Franklin and F. H. Field, *J. Am. Chem. Soc.* **76**, 1994 (1954).
- ²²⁰ A. J. B. Robertson, *Trans. Faraday Soc.* **48**, 229 (1952).
- ²²¹ Omura, Baba, and Higasi, *Bull. Chem. Soc. Japan* **28**, 147 (1955).
- ²²² J. L. Franklin and F. H. Field, *J. Chem. Phys.* **21**, 550 (1953).
- ²²³ N. I. Ionov, *DAN SSSR* **59**, 467 (1948).
- ²²⁴ T.-K. Liu and A. B. F. Duncan, *J. Chem. Phys.* **17**, 241 (1949).
- ²²⁵ T. M. Sugden and W. C. Price, *Trans. Faraday Soc.* **44**, 116 (1948).
- ²²⁶ W. C. Price and A. D. Walsh, *Proc. Roy. Soc. A* **179**, 201 (1941).
- ²²⁷ C. A. McDowell and B. C. Cox, *J. Chem. Phys.* **22**, 946 (1954).
- ²²⁸ H. Gutbier, *Z. Naturforsch.* **9a**, 348 (1954).
- ²²⁹ R. F. Baker and J. T. Tate, *Phys. Rev.* **53**, 683 (1938).
- ²³⁰ D. P. Stevenson and J. A. Hipple, *J. Am. Chem. Soc.* **64**, 2766 (1942).
- ²³¹ R. H. Müller and G. C. Brous, *J. Chem. Phys.* **1**, 482 (1933).
- ²³² A. G. Harrison and F. P. Lossing, *J. Am. Chem. Soc.* **82**, 1052 (1960).
- ²³³ V. H. Dibeler and R. M. Reese, *J. Res. Natl. Bur. Standards* **54**, 127 (1955).
- ²³⁴ J. D. Morrison, *J. Chem. Phys.* **19**, 1305 (1951).
- ²³⁵ W. B. Nottingham, *Phys. Rev.* **55**, 203 (1939).
- ²³⁶ J. Collin, *Bull. Soc. Chim. Belges* **62**, 411 (1953).
- ²³⁷ D'Or, J. Collin, *Bull. Soc. Roy. sci. Liège* **22**, 285 (1953).
- ²³⁸ R. J. Kandel, *J. Chem. Phys.* **23**, 84 (1955).
- ²³⁹ R. E. Fox and W. M. Hickam, *J. Chem. Phys.* **22**, 2059 (1954).
- ²⁴⁰ G. Nief, *J. Chem. Phys.* **48**, 333 (1951).
- ²⁴¹ H. Hartmann and H. Grunert, *Z. phys. Chem.* **199**, 259 (1952).
- ²⁴² O. Osberghaus, *Z. Physik* **128**, 366 (1950).
- ²⁴³ E. W. C. Clarke and C. A. McDowell, *Proc. Chem. Soc.*, 69 (1960).
- ²⁴⁴ H. D. Hagstrum, *Revs. Modern Phys.* **23**, 185 (1951).
- ²⁴⁵ E. C. G. Stueckelberg and H. D. Smyth, *Phys. Rev.* **36**, 478 (1930).
- ²⁴⁶ Friedman, Irsa, and Wilkinson, *J. Am. Chem. Soc.* **77**, 3689 (1955).
- ²⁴⁷ Burhop, Massey, and Watt, *The Characteristics of Electrical Discharges in Magnetic Fields*, Vol. 5, New York (1949), p. 145.
- ²⁴⁸ N. I. Ionov and M. A. Mittsev, *JETP* **40**, 741 (1961); *Soviet Phys. JETP* **13**, 518 (1961).
- ²⁴⁹ H. Neuert and H. Clasen, *Z. Naturforsch.* **7a**, 410 (1952).
- ²⁵⁰ W. C. Price and W. M. Evans, *Proc. Roy. Soc. A* **162**, 110 (1937).
- ²⁵¹ Takamine, Tanaka, and Iwata, *Sci. Papers Inst. Phys. Chem. Research (Tokyo)* **40**, 371 (1943).
- ²⁵² A. B. F. Duncan, *J. Chem. Phys.* **4**, 636 (1938).
- ²⁵³ Watanabe, Nakayama, and Mottl, *J. Quant. Spect. and Rad. Transfer* **2**, 369 (1962).
- ²⁵⁴ K. Watanabe and J. Mottl, *J. Chem. Phys.* **26**, 1773 (1957).
- ²⁵⁵ B. L. Kurbatov and F. I. Vilesov, *DAN SSSR* **141**, 1343 (1961), *Soviet Phys. Doklady* **6**, 1091 (1962).

Translated by M. V. King